

pubs.acs.org/JPCB Article

Charge Transport Measured Using the EGaIn Junction through Self-Assembled Monolayers Immersed in Organic Liquids

Yuan Li, Samuel E. Root, Lee Belding, Junwoo Park, Hyo Jae Yoon, Cancan Huang, Mostafa Baghbanzadeh, and George M. Whitesides*



Cite This: J. Phys. Chem. B 2023, 127, 407–424



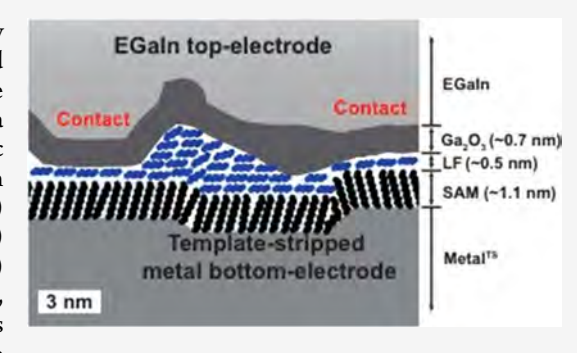
ACCESS I

III Metrics & More

Article Recommendations

s Supporting Information

ABSTRACT: This paper describes measurements of charge transport by tunneling through molecular junctions comprising a self-assembled monolayer (SAM) supported by a template-stripped metal bottom electrode (M^{TS}), which has been immersed in an organic liquid and contacted by a conical $Ga_2O_3/EGaIn$ top electrode. These junctions formed in organic liquids are robust; they show stabilities and yields similar to those formed in air. We formed junctions under seven external environments: (I) air, (II) perfluorocarbons, (III) linear hydrocarbons, (IV) cyclic hydrocarbons, (V) aromatic compounds, (VI) large, irregularly shaped hydrocarbons, and (VII) dimethyl siloxanes. Several different lengths of SAMs of n-alkanethiolates, $S(CH_2)_{n-1}CH_3$ with n = 4-18, and two different kinds of bottom electrodes (Ag^{TS} or Au^{TS}) are employed to assess the mechanism underlying the



observed changes in tunneling currents. Measurements of current density through junctions immersed in perfluorocarbons (II) are comparable to junctions measured in air. Junctions immersed in other organic liquids show reductions in the values of current density, compared to the values in air, ranging from 1 (III) to 5 orders of magnitude (IV). We interpret the most plausible mechanism for these reductions in current densities to be an increase in the length of the tunneling pathway, reflecting the formation of thin (0.5–1.5 nm) liquid films at the interface between the SAM and the Ga₂O₃/EGaIn electrode. Remarkably, the thickness of the liquid film—estimated by the simplified Simmons model, measurements of electrical breakdown of the junction, and simulations of molecular dynamics—is consistent with the existing observations of structured liquid layers that form between two flat interfaces from measurements obtained by the surface force apparatus. These results suggest the use of the EGaIn junction and measurements of charge transport by tunneling as a new form of surface analysis, with the applications in the study of near-surface, weak, molecular interactions and the behavior of liquid films adjacent to non-polar interfaces.

INTRODUCTION

Measurements of tunneling currents across insulating self-assembled monolayers (SAMs) supported by a template-stripped metal bottom electrode 1,2 (M^{TS}), with a eutectic gallium indium alloy ($Ga_2O_3/EGaIn$) top electrode—which we call "the EGaIn junction"—have been performed only under "dry" conditions, that is, with the junction formed in air, or some other dry gas. The ability to carry out measurements with the junction formed and immersed in a liquid would make it possible to study a range of interesting subjects (e.g., weakly bound complexes, biologically relevant systems, and wet-electrochemical gating).

This paper demonstrates that measurements of charge tunneling with the EGaIn junction can be carried out with the junction immersed in non-polar and low-polarity liquids. These demonstrations suggest, depending on the molecular nature of the liquid, the barrier through which charge tunnels can include one or more liquid layers. The phenomena we have observed correlate loosely with the studies of structured, near-surface liquids by Israelachvili^{10,11} and others^{12–20} who

observed oscillatory solvation forces. Measurements with the EGaIn junction will make it possible to explore, for example, problems ranging from the compactness (and thus, by inference, order) of the SAM to short-range (molecular scale) studies of interactions between SAMs and interacting liquids. We propose, based on these studies, that SAM-based molecular junctions formed in contact with organic liquids may provide what is, in effect, a new form of surface spectroscopy with three applications: (i) characterizing mechanisms of tunneling through SAMs, (ii) characterizing weak, reversible interactions at organic interfaces, and (iii) studying interactions between organic surfaces and unstructured or "loosely structured" organic liquids next to them.

Received: November 9, 2022 Revised: December 12, 2022 Published: December 29, 2022





To explore and characterize this new method, we must first address three basic questions. (i) Does charge tunneling through EGaIn junctions immersed in organic liquids involve only regions of contact between the SAM and the Ga₂O₃ skin of the EGaIn electrode or is there a mechanism in which the pathway of charge transport involves the organic liquid, by forming a liquid film that resists expulsion at the contacting interfaces? (ii) If the liquid does not directly contribute to the measured current by forming a surface film, does it change the charge transport characteristics of the SAMs by other interactions (e.g., by intercalation of the liquid into the SAM)? (iii) Does the effect of the organic liquid on the overall transport behavior of the junction depend on the interaction of the liquid with the surface film of Ga₂O₃, the chemical nature of the SAM, the MTS bottom electrode (through the supramolecular structure of the monolayer), or some combination thereof?

To address these questions, we focused on SAMs made from n-alkanethiols (SC $_n$) of variable length (n=4–18); we also used SAMs of polyfluorocarbons for a control experiment. The SAMs are formed on substrates made from template-stripped silver or gold (Ag^{TS} or Au^{TS}), which serve as bottom electrodes in junctions of the form of M^{TS}/SAM//organic liquid//Ga $_2$ O $_3$ /EGaIn, where "/" indicates a covalent bond and "//" indicates a non-covalent interaction.

When the junctions are formed under perfluorocarbon liquids, the influence of immersion is too weak to observe. In hydrocarbon liquids, however, the current densities decrease by factors of 10^2 to 10^5 , relative to junctions formed in air. These observed attenuations in current densities are compatible with the hypothesis that a thin film of liquid, which resists expulsion, forms at the interface between the surface of SAM and the Ga_2O_3 film of the EGaIn electrode. The inferred thickness of the liquid film (d_L, nm) is dependent on the structure of the liquid in ways that are consistent with the observations made by Israelachvili, Christenson, Klein, Heuberger, Benjamin, and others from surface force apparatus, $^{6-9}$ FT-IR, 14 XPS spectroscopies, 16,17 and simulations of molecular dynamics (MD). 18,19

EGaln Junction. This testbed for carrying out physicalorganic studies for molecular electronics has been developed and described extensively by us,³ Nijhuis,²² Chiechi,²³ and others (Yoon,²⁴ and Thuo²⁵). As typically used, a shaped tip of eutectic gallium-indium alloy (EGaIn) covered with a spontaneously formed film of electrically conductive metal oxide (represented approximately as Ga_2O_3) is contacted with a SAM supported on thin (~300 nm) films of templatestripped (TS) gold or silver surfaces on glass. It is relevant for this work that both the Ga₂O₃ layer and the M^{TS}/SAM have structural roughness on scales ranging from nanometers to micrometers, and the region of contact through the interface of tip/SAM contact should probably be thought of as an array of micro-/nanoelectrodes, rather than a region of continuous electrical contact.^{26,27} The current density through the observable region of contact is only a fraction (10⁻⁸ to 10⁻⁴) of that observed for largely conformal junctions, for example, evaporated metal or mercury drop, which are themselves not perfectly conformal.^{28,29}

Although the EGaIn junctions are remarkably consistent and reproducible within a set of parameters—a fact that is especially important for physical-organic studies, such as in this work—the influence of the contributions from each component of the junction needs to be considered to interpret

the experimental results. For instance, the structures of SAMs, the interfaces between SAMs and electrodes, and the physical properties of electrodes are all reasonably defined. $^{3,4,26,28,30-34}$ The influence of the footprint of the contact is reproducible and consistent but can differ in some details in the approach used for their fabrication among groups. Measurements using the EGaIn junction are normally performed in ambient condition (room temperature, air, or dry N_2), and a change of humidity from \sim 45 to 10% does not result in a significant difference in current densities through SAMs of Au^{TS}/SC_n .

Structure of Liquid at Interfaces. The inference by Israelachvili and co-workers of structured thin films (<5 layers) of organic liquids at the flat interfaces of the surface force apparatus (SFA) changed the understanding of molecular physics at solid—liquid interfaces. ^{10,11,35,36} Molecules with low molecular weight in the liquid state form structured liquid films between two mica surfaces, two metal surfaces, or mica and metal surfaces. ¹⁰

SFA experiments¹⁰ showed that, when two flat interfaces are brought into contact with both immersed in a solvent, the measured force versus distance curve oscillates with a periodicity corresponding to the length of the shortest axis of the molecules making up the solvent. These oscillations result from the formation of ordered molecular layers at flat, solid interfaces and are predominately geometric in origin (i.e., are mainly due to the excluded volume and not the intermolecular forces; see Supporting Information S1 for a more detailed description). The thickness and structure of the ordered liquid film depend on the shape of the molecules making up the liquids and, in most cases, are a multiple of the shortest axis of these molecules. Thompson and Robins used MD simulations of liquid (between two flat, gold plates) to support the inference that hexane and benzene molecules are oriented at a flat, solid interface. 37,38

Previous studies with SFA have also examined the interactions of organic liquids with SAMs. Christenson and Claesson used their modified SFA system to show that liquid (e.g., hexane, decane, and hexadecane) films form at the interface between an alkanethiol SAM (Au-SC14) and a mica surface. 13 Klein et al. have shown that layers of water are formed between an alkanethiol SAM (Au-SC₁₀) and a mica surface. 15 These studies (and others 40) provide evidential background to the work we present but differ in at least four ways (and thus provide four key components to consider in our system): (i) surface roughness: mica, gold, and SAMs are assumed to be flat, while the EGaIn/Ga₂O₃ surface is rough (at the nanoscale and probably the microscale). (ii) Surface energy: gold, silver, and Ga2O3 all have high interfacial surface energies; the SAMs we examined, in general, have a low surface energy. (iii) Dynamics: bulk movement of solvent at the interface, and time-dependent rearrangement (on the scale of microseconds) in liquid structure seem not to be important in our system. Previous work has suggested that in Hg/SAM// SAM/Hg junctions, 41 hexane forms thicker liquid layers at the SAM//SAM interface than ethanol. This observation suggests that bulk dynamics of the liquid can be important in certain circumstances, depending on some physical property of the liquid (e.g., polarity, strength of intercalation, interaction in the liquid, and dielectric constant).

Tunneling Junctions Immersed in Liquid. Existing studies of tunneling across junctions involving SAMs in contact with liquids do not resemble SFA studies. Three techniques have previously been employed to investigate the influence of

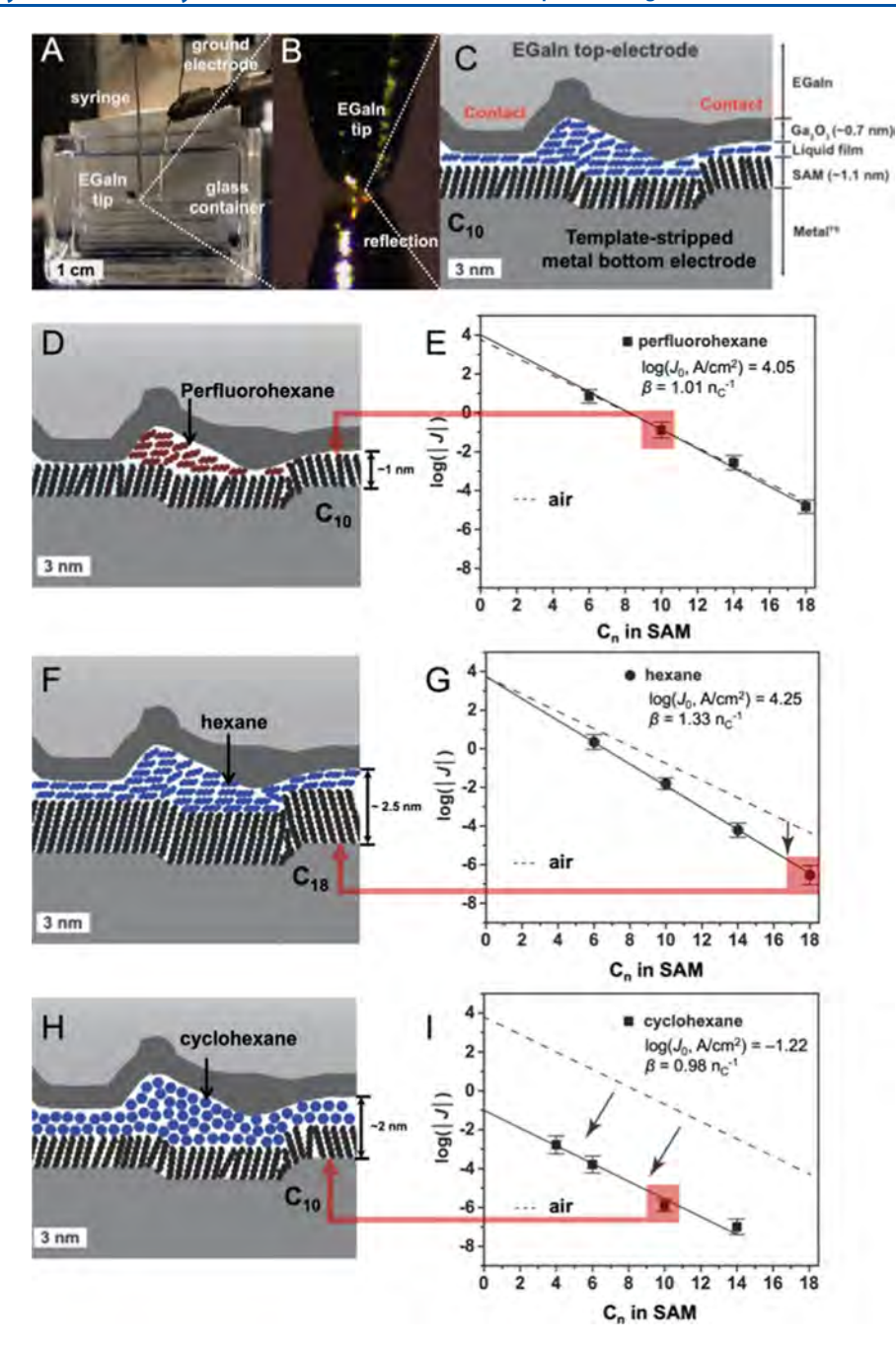


Figure 1. Measurements with the EGaIn junction immersed in organic liquids. (A) Photograph, (B) microscopic image, and (C) schematic diagram of an EGaIn junction with the structure: $M^{TS}/SAM//organic liquid//Ga_2O_3/EGaIn$. Schematic diagram (D) of the junction containing SAMs of C_{10} , immersed in perfluorohexane, as well as the corresponding plot (E) of the Gaussian mean values of log(|J|) at -0.5 V vs the number of carbon atoms, n, in a SAM of $Ag^{TS}-S(CH_2)_{n-1}CH_3$. ("—" indicates that the EGaIn electrode is at a negative voltage—that is, the EGaIn electrode is reducing relative to the bottom metal electrode, which is grounded). Schematic diagram (F) of the junction containing SAMs of C_{18} , immersed in hexane, and the corresponding plots (G) of the Gaussian mean values of log(|J|) vs the number of carbon atoms, n. Schematic diagram (H) of the junction containing SAMs of C_{10} , immersed in cyclohexane, and the corresponding plots (I) of the Gaussian mean values of log(|J|) vs the number of carbon atoms, n. The dashed lines are the values of log(|J|) measured in air. The schematic diagrams are approximate representations in two dimensions of inferences from experiments and observations from MD simulations.

solvents on tunneling through molecules: scanning tunneling microscopy (STM), ⁴² STM break junctions, ⁴³ and mechanical break junctions. ⁴⁴ Tao et al. used STM break junctions with solvents of different characteristics to infer that contacting liquids do not contribute significantly to the measured conductance of fully saturated molecules, such as alkanedithiols in the STM break junction. ⁴⁵ In contrast, Tao and Venkataraman measured changes (both increases and

decreases) in conductance in STM break junctions,⁴⁶ in contact with polar liquids (i.e., 1,2,4-trichlorobenzene or 1-bromonaphthalene), which they claimed to result from (or correlate with) molecules having delocalized orbitals (e.g., polyacetylene with the arylthiomethyl group as the anchor group). (ii) SAM-based tunneling junctions can be prepared by techniques that include direct-deposited metals,⁴⁷ liquid metals (Hg or EGaIn),^{3,41} graphene,⁴⁸ conductive polymer,⁴⁹

or nanoparticles. Only the Hg-drop double-layer junction (i.e., Hg(or Au)- SC_n // C_nS -Hg junctions) has been used to measure the charge transport through two layers of SAMs immersed in liquid (ethanol and hexane). Capacitance measurements of such double-layer junctions showed an increase in capacitance when SAMs of alkanethiolates were immersed in hexane, and this observation was interpreted to suggest that the tunneling distance increased due to the trapping of molecules between the SAMs.

Simplified Simmons Equation. We use the simplified Simmons equation (eq 1) to characterize and compare charge transport across junctions in contact with air or liquid as a function of alkyl chain length of the molecules in the SAM

$$J = J_0 e^{-\beta d} \tag{1}$$

Here, β ($n_{\rm C}^{-1}$ or ${\rm \AA}^{-1}$) represents the tunneling decay coefficient, which is related to the mean height of the tunneling barrier with an assumed rectangular shape; d (n or Å) represents the width of the tunneling barrier; and I_0 (A/ cm²) represents the "apparent injection current density" when J(V) is extrapolated to d=0. The Simmons equation, as Simmons⁵³ and many others^{54,55} have noted, is internally inconsistent and is not appropriate for detailed quantum mechanical treatment of transport data. The simplified Simmons equation does, however, provide a very useful and widely employed empirical interpretation of empirical results: it describes a large number of systems involving tunneling and facilitates comparison among literature data. 5,56,57 The experimental values of β deduced from many studies of nalkanethiolate SAMs are close to 1.0 $n_{\rm C}^{-1}$ (~0.8 Å⁻¹);^{5,28,55} the values of J₀ differ by approximately 12 orders of magnitude depending on the experimental systems.^{5,55,58-61} In a given system, and especially in the one used here, the values are very reproducible. 28,3

Here, we demonstrate that the influence of a liquid contacting the electrically conducting region of the junction on measurements of J ranges from "no effect" to a substantial decrease ($\sim 10^2$ to 10^5) in tunneling current densities. The values of β can also increase when the junction is measured in liquid. We have not, however, observed a contacting liquid that increases the values of J(V) for a junction immersed in that liquid relative to that junction in air.

Junctions Immersed in Organic Liquids. Figure 1A–C shows photographs and schematically illustrates the EGaIn junction in contact with liquid, summarizing our hypothesis that a liquid film forms at the SAM//Ga₂O₃ interface. If the film forms, the total tunneling distance (d, nm) would be the sum of the thickness of the SAM $(d_{\text{SAM}}, \text{nm})$ and the thickness of the liquid film $(d_{\text{LF}}, \text{nm})$. Figure 1D–I shows the dependence of $\log(J)$ on the number of carbons in the SAM of alkanethiolates immersed in perfluorohexane (Figure 1D,E), hexane (Figure 1F,G), and cyclohexane (Figure 1H,I); the dashed line represents the data measured in air, and the solid line is the data measured in liquids, fit to the Simmons equation. In these experiments, we observed three types of tunneling behaviors:

i Figure 1E presents the values of log(J) and β (the slope), for n-alkanethiol SAMs measured in perfluor-ohexane. These data are indistinguishable from the analogous junctions measured in air. We interpret these data to mean that the barriers to tunneling in these experiments are equal and that the perfluorocarbons

- therefore do not interact with the exposed hydrocarbon (specifically, $-CH_3$ groups) surface of the SAM or the Ga_2O_3 . Considering the very weak interactions of perfluorocarbons with hydrocarbons, ⁶² these observations are not surprising.
- ii Measurements of n-alkanethiol SAMs in n-hexane are compatible with the hypothesis that there has been an apparent increase in the width of the tunneling barrier which is proportional to the increase in the thickness of the SAMs (Figure 1G). The measured value of |J| for C_{10} in contact with n-hexane is approximately the same as measured for C_{13} in contact with air. The contact with nhexane (in this case) adds an apparent thickness of C₃ (i.e., three carbons, ~ 0.35 nm) to the thickness of the barrier (assuming that its height remains effectively unchanged). Comparison between the measured values of the tunneling decay coefficient, β , for experiments in *n*-hexane and in air indicates that $\beta_{n\text{-hexane}}/\beta_{\text{air}} \approx 1.3$. This result is compatible with two hypotheses: either (i) the thickness of the liquid film increases with the length of the alkyl chains in the SAM or (ii) the extent to which the n-hexane intercalates into the SAM increases with the length of the alkyl chains in the SAMS. Our detailed results from further experiments and simulations (described below) suggest the former mechanism (i); however, the latter mechanism (ii) cannot be entirely ruled out based on the existing evidence and would require further investigation.
- iii Cyclohexane produces a qualitatively different behavior compared to hexane. The value of β for the nalkanethiolate SAM immersed in cyclohexane is indistinguishable from that of air, but the value of logl J_0 changes from 3.8 (in air) to -1.0 (in cyclohexane). Thus, while the two lines (Figure 1I) are parallel, the apparent width of the barriers for experiments in cyclohexane is approximately equivalent to an increase of 11 CH₂ groups (or $d \sim 1.27$ nm) compared to that in air. The immediate interpretation of these observations is that there is a surface-associated liquid film with a thickness corresponding to a few (~ 2) layers of cyclohexane, which resists expulsion from the region between the SAM and the surface of the Ga₂O₃/EGaIn electrode (Figure 1H). We estimate the thickness of a cyclohexane film from the mean intermolecular separation of cyclohexane molecules in its crystalline state $(\sim 3.2 \text{ Å})^{63}$ and from our MD simulations (see the MD Simulations section).

We will discuss these results in greater detail in the Results and Discussions section. Briefly, it seems that the liquid in which the junction is immersed does interact with the SAM, but the interaction depends on the thickness of the SAM, the type of the bottom electrode (Ag^{TS} or Au^{TS}, which influences the structure of the SAM), and the molecular structure of the contacting liquid.

■ EXPERIMENTAL DESIGN

Selection of Bottom Electrodes. Gold (Au) and silver (Ag) are the two most commonly used metals for fabricating electrodes for SAM-based tunneling experiments since they are easily and reproducibly prepared as flat surfaces (root-mean-squared roughness < 0.5 nm) and form stable covalent bonds with the sulfur atoms of organic thiols.⁶⁴ The difference

between a Au–S (sp² hybridization) and Ag–S (sp hybridization) bond affects the packing structures of *n*-alkanethiolates. In particular, Schlenoff⁶⁵ and we³⁹ have reported that *n*-alkanethiolate SAMs formed on Au have 10% lower surface coverage than those formed on Ag. We use both Au and Ag as bottom electrodes to examine whether the charge transport through SAMs under liquid depends on the structure of the bottom electrode (i.e., in principle, both the M–S interface and the structure of the packing and the SAM). We conclude from the information in the following sections that the metal–sulfur interface does not affect the structure of the ordered liquid layer.

Selection of SAMs. Charge transport measurements through SAMs of n-alkanethiolates (SC $_n$) with different molecular lengths are usually used as an internal standard to establish the quality of a new type of junction. They also form a consistent standard for related sets of experiments, such as immersing the junction under different liquids, as reported here. In particular, the tunneling decay constant can be used to assess reproducibility and provide comparisons with measurements made with other approaches using different top contacts (e.g., Hg-drop, graphene, and conducting atomic force microscopy). 28,48,55

We measured charge transport through polyfluorinated SAMs of Ag^{TS} -S(CH₂)₂(CF₂)₇CF₃ under a variety of nonpolar liquids as a control experiment to isolate contributions from interactions between the liquid and the monolayer or the liquid and the EGaIn electrode. We expected that hydrocarbon liquids would not interact with the fluorinated SAMs, and thus, any change in current density would result from interactions between the liquid and the surface of the Ga₂O₃/EGaIn electrode.

Selection of Liquids. In order to understand the relationship between the molecular structure of the organic liquid under which the junctions were formed and charge tunneling, we have conducted measurements in seven types of environments: (I) air, as a control experiment; (II) perfluorocarbons, for example, perfluorodecalin and perfluorohexane, liquids that we assume do not strongly interact with SAMs of SC_n; (III) linear hydrocarbons, for example, hexadecane (which has long alkyl chains), decane (which is intermediate in length), and hexane (which is shortest); (IV) cyclic hydrocarbons of differently sized rings (e.g., cyclohexane, cyclooctane, cyclohexene, and cyclooctadiene); (V) aromatic compounds (e.g., benzene, toluene, and hexyl benzene) which we assume might have a lower total tunneling decay coefficient due to the delocalized π -electrons; (VI) large molecules with complex shapes (e.g., diphenylmethane, cis-decalin, transdecalin, tran,tran,cis-1,5,9-cyclododecatriene, and methylcyclopentadiene dimer) which we assume (based on SFA measurements¹⁰) inhibits the formation of a structured liquid layer; and (VII) dimethyl siloxanes in linear and cyclic structures (which are non-polar but have a -(Si-O)backbone rather than a -(C-C)- backbone) which are more flexible than the corresponding hydrocarbon molecules. This set of liquids was chosen to elucidate the role of molecular size and shape and intermolecular forces on the variations in tunneling current density.

Formation of EGaIn Junctions Immersed in Liquids. The procedure for forming EGaIn tips in air has been extensively described elsewhere. The procedure used here is similar. We begin with a sacrificial bare template-stripped (TS) Au^{TS} (or Ag^{TS}) surface freshly cleaved from the Si/SiO₂

(111) surface against which it is formed by electron beam evaporation of metal. An approximately spherical drop of EGaIn is then extruded from a 10 μ L syringe (Hamilton) with a stainless steel needle under air. We use a micromanipulator, which holds the syringe, to bring the drop of EGaIn into contact with the Au^{TS} (or Ag^{TS}) surface, which it wets and to which it spontaneously adheres. We then pull the syringe away from the surface. The EGaIn elongates into the shape of an hourglass and finally breaks at the thinnest region of the neck. This process generates a conical tip with a radius of contact of $10-20 \mu m$. To form EGaIn junctions in liquid, we use the micromanipulator to bring this freshly made EGaIn tip into a rectangular glass container (~10 mL in volume) containing the liquid of interest, with the SAM $(M^{TS}-SC_n)$ in it. We do not flatten the tip prior to forming the contact with the SAM because the process of tip-flattening can contaminate the surface of the tip by physisorption of dust and other impurities.³⁰ To confirm that the EGaIn tip is in physical contact with the SAM, we use a microscope connected to a CCD camera to observe the deformation of the EGaIn tip when it comes into contact with the SAM. This type of visual observation might be subjective, but we keep it consistent with the procedure used for the formation of EGaIn junction in air (see Figure 1A,B for the images of junctions under liquid). This procedure allows us qualitatively to estimate that the contact area on the interface of tip/SAM in liquid is comparable to that at the same interface in air that we have reported before.²⁶

Dynamic Range of the Electrometer. This work involved measuring small tunneling currents across electrically resistive SAMs, and we were thus concerned with the dynamic range of the electrometer. The lower limit of current detection for a Keithley 6410 electrometer is 0.1 fA. Due to the noise from the connection of cables and magnetic interference from the environment, the lowest current we can measure is approximately ~ 0.1 pA (current density = $J \sim 10^{-8}$ A/cm² with an area of contact of $\sim 1000 \ \mu \text{m}^2$, using our conical EGaIn tip). The junctions immersed in cyclic hydrocarbons yield lowest values of J among junctions in all liquids. The lowest values of J (±0.5 V) we measured with SAMs of C₁₆ in cyclohexane is only 10× greater than the detection limit ($I \sim$ 10^{-8} A/cm²). We cannot measure any reasonable J(V) signal (only random fluctuations of J at $\sim 10^{-8}$ A/cm² as a function of V) for junctions with SAMs of C₁₈ (either on Ag^{TS} or Au^{TS}) in liquids of cyclic hydrocarbons.

Simulation of the Structure of EGaIn Junctions Immersed in Liquids by MD. To provide insights into the structure of the liquid films in the junctions and visualization to help understand and describe the molecular mechanisms responsible for the observed change in tunneling currents, we performed atomistic MD simulations of a selected set of solvents and SAMs. Due to the absence of parameters that describe the pairwise interactions of the atoms in the EGaIn tip with the organic molecules of the SAMs, we have instead used a block of gold Lennard—Jones atoms. These simulations are thus meant to illustrate qualitatively what might be happening at the interface as the EGaIn tip contacts the SAM. The simulations were run by applying a fixed pressure to the gold slab and observing the resulting equilibrium structure. Details of the simulation methods are given below.

EXPERIMENTAL METHODS

Formation of SAMs. We used ultra-flat template stripped metal (Ag^{TS} or Au^{TS}) substrates with a root-mean-square surface roughness of $\sim 0.5-0.6$ nm for Ag^{TS} and $\sim 0.4-0.5$ nm for Au^{TS} (see the Supporting Information for the preparation of TS substrates). We cleaved the metal substrate from the Si wafer in air and immediately (~ 5 s) immersed it in a 1.0 mM solution of thiols dissolved in anhydrous ethanol. The sample was incubated for 3 h at room temperature to allow for the formation of a SAM—during this time, a needle attached to a balloon filled with N_2 was inserted into the septum that sealed the vial to ensure positive pressure of an inert atmosphere inside the container (these systems are not particularly sensitive to oxygen). After the formation of the SAMs, the substrates were rinsed gently with ~ 20 mL of ethanol and dried in a stream of N_2 gas.

Electrical Characterization. We measured J(V) by charge tunneling across the SAMs with the junction in air (as a reference) and with the junction immersed in liquids. Our experimental procedure has been described previously:^{28,30} we grounded the Au or Ag bottom electrodes with a gold probe that penetrated the SAM; the top electrode of Ga₂O₃/EGaIn was biased from 0 V \rightarrow 0.5 V \rightarrow 0 V \rightarrow -0.5 V \rightarrow 0 V, with a step size of 50 mV (i.e., ten 50 mV steps between 0 and 0.5 V), and a 0.1 s delay at each step. We carried out the following types of experiments to facilitate comparisons. (i) We measured the junctions of AgTS-SC10 in all liquids, compared the log(IJI) against different liquids, and sorted the liquids into seven different contacting fluids (including air). (ii) We carried out more extensive studies to determine the values of β and I_0 using SAMs of SC_n immersed in several liquids representing different electrical and molecular classes: perfluorocarbons, linear hydrocarbons, and cyclic hydrocarbons. (iii) We also compared the values of log(IJI) measured on the SAMs of $S(CH_2)_2(CF_2)_7CF_3$ to that of SC_{10} immersed in six liquids from the seven classes of media.

To study the dynamics of the interaction of the EGaIn tip with the SAM in contact with the liquids, as well as the stability and reproducibility of these junctions, we performed four additional kinds of experiments (Supporting Information S3): (i) we immersed freshly cleaved AuTS surfaces (i.e., immediately after separating the Au^{TS} surfaces from the surface of the silicon wafer) in hexane or cyclohexane and then brought the EGaIn tip into contact. We found that all junctions formed this way exhibited electrical shorts. (ii) We measured tunneling currents through junctions of SAMs of Ag^{TS}-SC₁₀ that were formed in air and then subsequently immersed in hexane (by slow injection of the liquid into a 5 mL glass container, ~1 mL/min), and we did not observe statistically significant changes in the values of J. (iii) We carried out 1000 replicate traces in one junction (SAMs of C₁₀ immersed in hexadecane) and did not observe any statistically significant changes log(|J(+1.0 V)|) over the course of these measurements; all measured values were within 1 standard deviation of $\sigma_{\log I} = 0.3 \log(A/cm^2)$ obtained from the standard protocol including seven distinct junctions and 20 scans per junction. This observation indicates that the junctions are stable against electrical shorts under an applied voltage of 1.0 V. (iv) We examined tunneling through junctions of SAMs of AgTS-SC10 that had been removed from hexane, cyclohexane, or benzene, after allowing the liquids to evaporate from the surface of the SAM in air. We compared the results of these experiments with

junctions of SAMs that had not been immersed in liquids and observed no differences in *I*.

Measurements of Electrical Breakdown. The mechanism of electrical breakdown of SAM-based junctions has been examined by Cahen,⁶⁷ Nijhuis,⁶⁸ and us.⁴¹ This breakdown involves the electromigration of metal atoms from the bottom electrode to the EGaIn tip. The electromigration generates conducting structures that penetrate the SAM form micro-/ nanofilament bridges and result in electrical shorts between one electrode and the other. 41,68-70 This mechanism does not seem to include the dielectric breakdown of the SAM because the breakdown electrical field (E_{bd}) depends strongly on the nature of the bottom electrode rather than the SAM. 41,68-70 Based on this mechanism, we assume that $E_{\rm bd}$ is the same for the junctions formed under organic liquids, and we can thus estimate the thickness of a dielectric layer between the two electrodes based on a measured breakdown voltage $(V_{\rm bd})$. It is possible that the presence of structural defects in the SAM could have an effect on $E_{\rm bd}$, but all existing evidence suggests that such effects are less important than the nature of the electrodes. 41,68-70 We have reported that eq 2 describes the electric field required for electrical breakdown.

$$E_{\rm bd} = V_{\rm bd}/d \tag{2}$$

where d is the width of the insulating tunneling barrier and $V_{\rm bd}$ is the applied voltage (in our case, it is the voltage applied to the EGaIn electrode relative to the grounded bottom electrode) between two electrodes when the junction shorts. Experimentally, the values of $V_{\rm bd}$ increase with the thickness of the SAMs. Au-SC $_n$ //C $_n$ S-Hg (n=5-20) junctions show a linear dependence of $V_{\rm bd}$ as a function of d with a slope. The value of breakdown electrical field estimated from this procedure is $E_{\rm bd}\cong 0.85$ GV/m. Nijhuis et al. report similar values ($E_{\rm bd}\cong 0.81$ GV/m) with junctions of the form Ag^{TS}-SC $_n$ //Ga $_2$ O $_3$ /EGaIn.

It is not possible to observe the liquid film in situ by spectroscopy or microscopy. Therefore, we apply measurements of electrical breakdown to estimate the thickness of the liquid film based on the fact that materials with a similar electrical dielectric constant break down under similar electrical fields, for example, for a polyethylene film, $E_{\rm bd}$ = 0.6–0.8 GV/m. ⁴¹ We hypothesize that the thickness of a liquid film incorporated into a junction (Ag^{TS}-SC_n/organic liquid/ Ga₂O₃/EGaIn) can be approximated by measuring the breakdown voltage of the junctions immersed in the liquid. With this approach, d would be the sum of the thickness of the SAM (taken as the length of the molecule), and the thickness of any liquid film (measured perpendicular to the mean surface of the electrode) between the "top" of the SAM and the surface of the Ga₂O₃. We note that this approach for inferring the thickness of the junction relies on the assumption that the voltage drop per unit length is the same for the liquid layer and the SAM. Since we expect the voltage drop to be slightly steeper across the liquid layer based on the difference between "through bond" and "through space" tunneling, 71 the thickness estimated in this way represents an upper bound for the actual thickness.

MD Simulations. All MD simulations were run using LAMMPS and visualized using OVITO. The initial conditions for the MD simulations were prepared by arranging 256 equally spaced molecules, at a density of 22.6 Å²/chain, on a gold (111) slab. Next, 1000 solvent molecules were randomly deposited above the monolayer. The simulation was specified

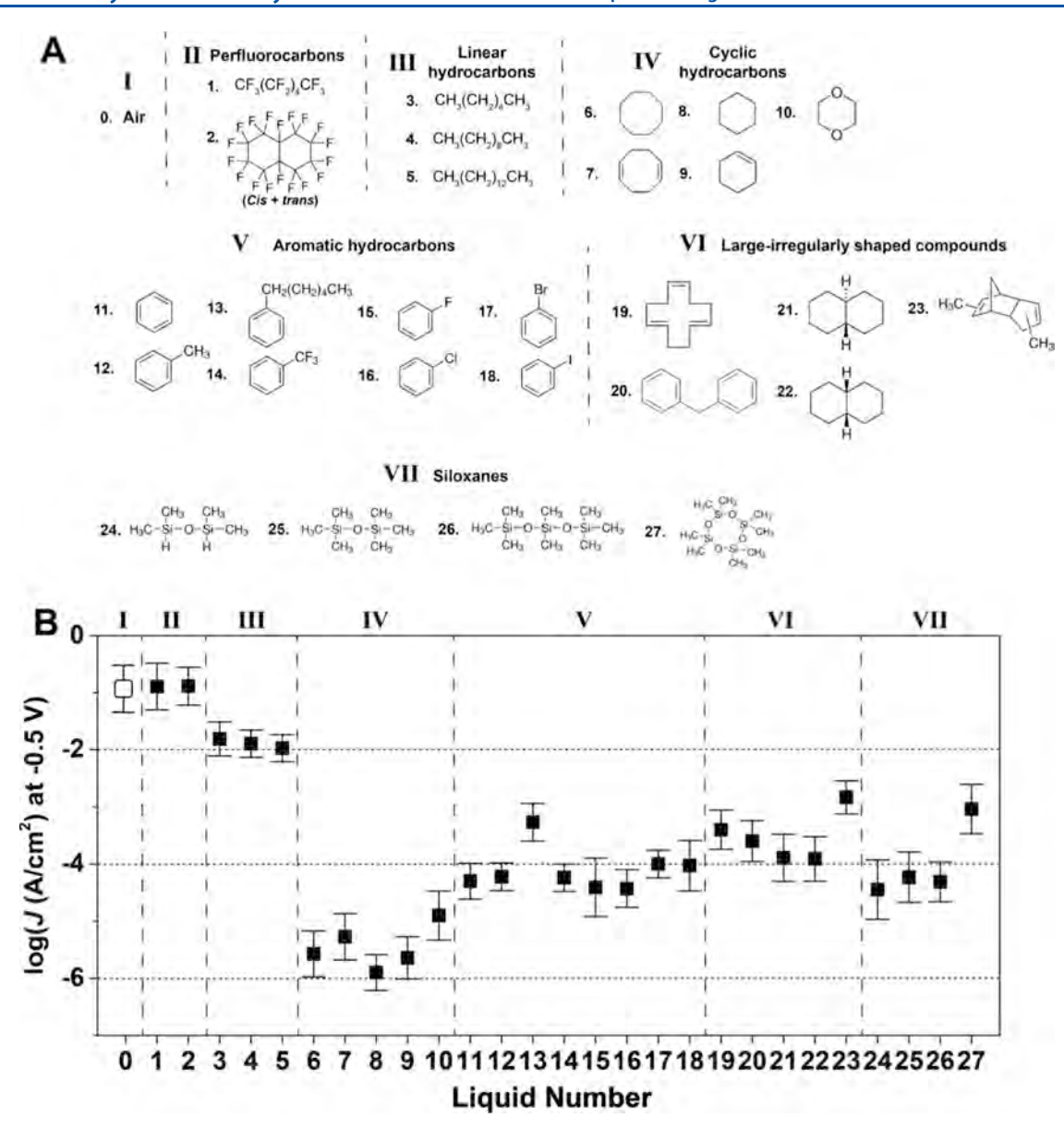


Figure 2. Survey of the effects of different organic liquids. (A) Molecular structures of organic liquids studied in this work. (B) Values of $\log(|JI|)$ at -0.5 V through junctions of the form ${\rm Ag^{TS}/SC_{10}//organic}$ liquid// ${\rm Ga_2O_3/EGaIn}$. The x-axis corresponds to the number listed in (A). The plot is separated into seven different regions by the types of solvent: air (I), perfluorocarbons (II), linear hydrocarbons (III), cyclic hydrocarbons (IV), aromatic hydrocarbons (IV), large compounds (VI), and siloxane (VII).

with periodic boundaries in the x, y dimensions and fixed boundaries in the z dimension (box dimensions, $81 \times 70 \times 70$ 140 Å³). Dynamics were run using the GAFF force field,⁷⁴ which includes Lennard-Jones plus electrostatic pairwise interactions, harmonic bond and angle potentials, and dihedral potentials described by a Fourier series. Lennard-Jones interactions were truncated and shifted to zero at a cutoff radius of 12 Å. Long-range electrostatic interactions in the x, ydimensions were treated using an Ewald summation to a specified force accuracy of 1×10^{-4} kcal/mol Å. Due to the quasi-2D nature of the system, long-range electrostatic forces in the z dimension were set to zero. Parameters specific to the gold-sulfur interactions were taken from the work of Ghorai and Glotzer;⁷⁵ the gold-sulfur bond was treated with a pairwise additive Morse potential. Once the initial conditions were specified, we ran a conjugate gradient energy minimization. Subsequently, the system was thermalized

using a Nose–Hoover thermostat (time constant = 100 fs) that increased the temperature from 0 to 400 K over the course of 5 ns, using a timestep of 1 fs. We ran dynamics at 400 K for 10 ns, cooled the system to 300 K over 5 ns, and then equilibrated the system at 300 K for 5 ns. For the production runs, a rigid slab of gold was placed in the vacuum region above the solvent and then pushed toward the surface at a fixed rate of displacement of $10 \, \text{Å/ns}$. When the gold slab was in the vicinity of the surface (3 nm), a constant downward pressure of $10^5 \, \text{kPa}$ was applied to the gold slab, and the simulation was allowed to come to equilibrium over the course of 10 ns.

■ RESULTS AND DISCUSSION

Comparison of the Junctions of SC₁₀ Immersed in Liquids. We begin our discussion with a survey of the effects of different organic liquids (Figure 2A) on the tunneling currents through EGaIn junctions of the form Ag^{TS}/SC₁₀//

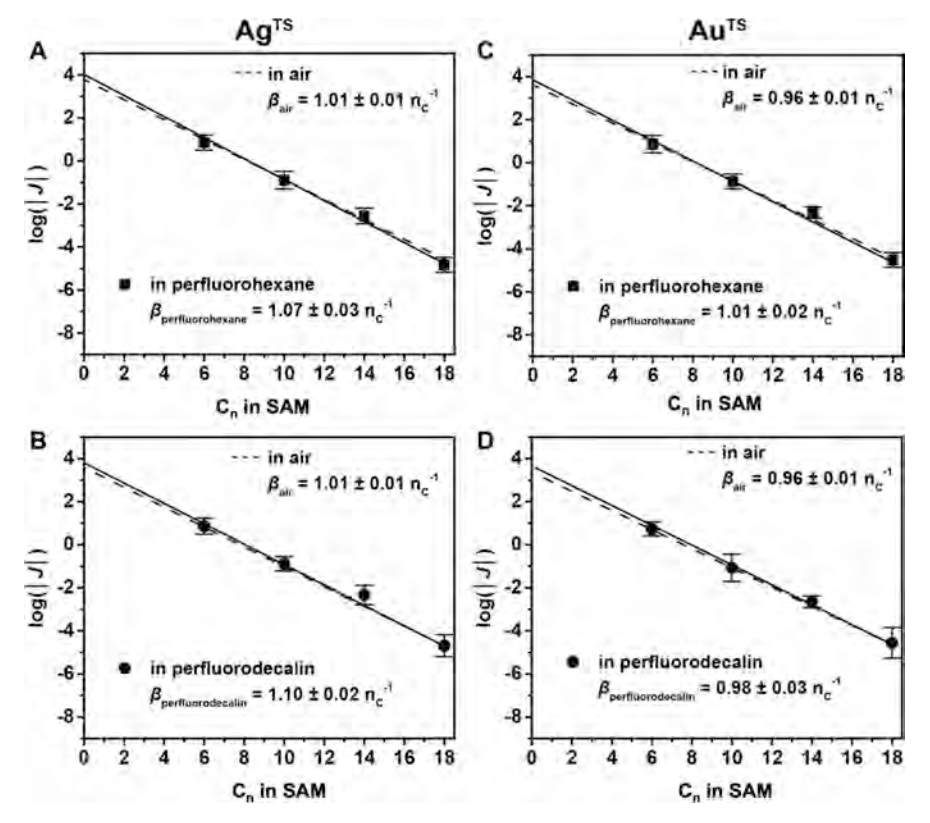


Figure 3. Plots of the Gaussian mean values of log(|J|) at -0.5 V against the number of carbon atoms in the alkanethiol, C_n . The dashed lines are the log(|J|) measured in air and the solid squares or circles are measured in either perfluorohexane (A,C) or perfluorodecalin (B,D). The error bars represent the standard deviation of the Gaussian mean values (for details of measurements and analysis, see the Supporting Information). The solid lines are the Simmons equation (eq 1) fit to the solid squares or circles.

organic liquid// Ga_2O_3 /EGaIn. The measured values of log(I J(-0.5 V)I) under organic liquids of different molecular structures are shown in Figure 2B. We partitioned the data into seven sets, corresponding to seven different types of environments: (I) air, (II) perfluorocarbons, (III) linear hydrocarbons, (IV) cyclic hydrocarbons, (V) aromatic compounds, (VI) large, irregularly shaped compounds, and (VII) siloxanes.

Compared to control experiments performed in air, the current densities measured in organic liquids ranged from "no change" in perfluorocarbons (II) to "reductions of 5 orders of magnitude" in cyclic hydrocarbons (IV). The current densities measured under liquids of perfluorocarbons suggest that these molecules do not interact with any of the components of the junction, either by intercalation into the SAM or by adsorption to the surface of Ga₂O₃ or the SAM. This result is not surprising, given the weak intermolecular interactions between alkanes and perfluorocarbons. In contrast, the results obtained from the various hydrocarbon liquids of different sizes and shapes are consistent with what would be expected from the formation of liquid films between the SAM and Ga₂O₃ interfaces that resist expulsion upon formation of the junction.¹⁴

The structure of ordered liquid films at solid—liquid interfaces is known from SFA measurements to depend sensitively on the shape of the molecules comprising the liquid (assuming that all other relevant factors such as surface roughness and chemistry are held constant, as is the case with these experiments). In general, spheroidal molecules form liquid films with longer range order and more pronounced oscillatory solvation forces (i.e., higher amplitudes and more

repeating periods) than irregularly shaped molecules.¹⁰ This general picture is consistent with our observations that linear hydrocarbons (II) yield much smaller reductions in current than cyclic hydrocarbons (III). Although these molecules are similar in the size of their shortest molecular axis, the asymmetric shape of linear alkanes would be expected to form less-ordered liquid films. Moreover, considering the results from the aromatic hydrocarbons (IV), we observed that molecules of similar shape (11-18, except for 13) gave similar reductions in current density. The single outlier from group IV was hexylbenzene (13): the only molecule in the group containing a flexible alkane side chain, which would be expected to frustrate the formation of ordered structures. The observation that cyclic hydrocarbons (III) yield much larger reductions in current densities than large, irregularly shaped hydrocarbons (VI) suggests that multiple solvation layers must be present in liquid films of group III, as each layer of molecules from group VI would be expected to have a more pronounced effect on the current density than smaller cyclic hydrocarbons of group III. Siloxanes (VII) produced reductions in the I intermediate between the reductions in I from linear (III) and cyclic (IV) hydrocarbons. These results suggest the formation of monolayers of liquid. Because 27 is a larger molecule (in terms of the length of the shortest axis of the molecule) than 24-26, it was surprising that junctions measured in molecule 27 showed a higher current density than molecules 24-26. We do not understand the physical mechanism underlying this observation.

Chain Length Dependence of SC_n SAMs in Organic Liquids. While the single-point current density data presented

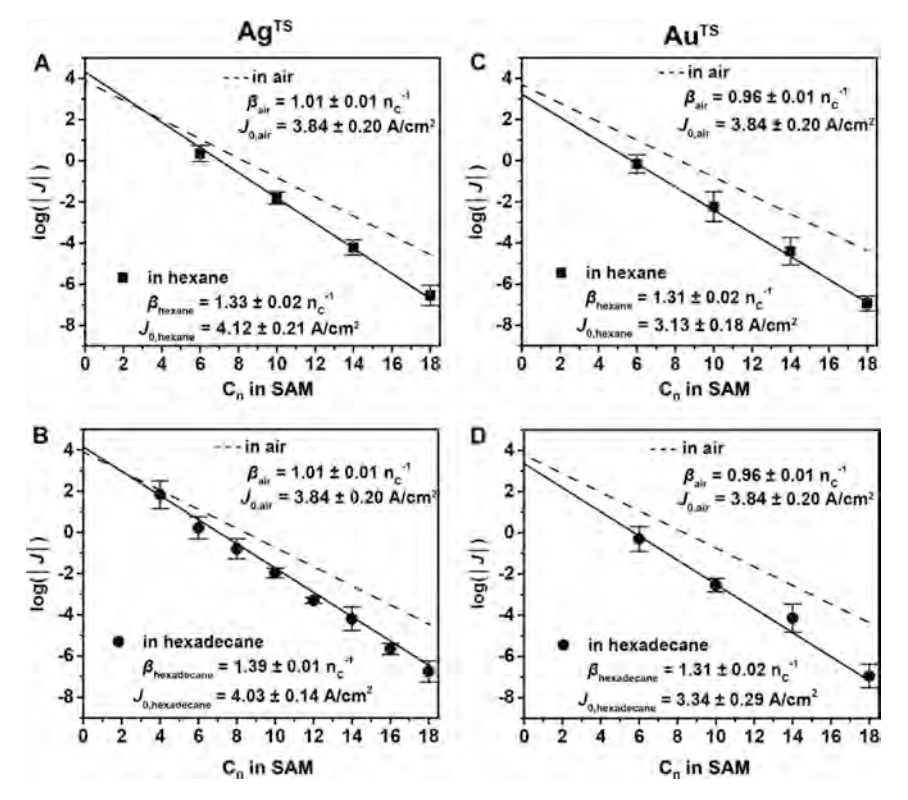


Figure 4. Plot of the Gaussian mean values of log(|J|) at -0.5 V against the number of carbon atoms in the molecules of the SAM. The dashed lines best fit from the log(|J|) measured in air, and the solid squares are those measured in either hexadecane (A,C) or hexane (B,D). The error bars represent the standard deviation of the Gaussian mean values, and the solid lines are the fit of the data to the Simmons equation (eq 1).

in Figure 2 allowed for a preliminary comparison of the effects of structure of different organic liquids on the charge transport characteristics of the junctions to build a more detailed understanding of the mechanisms involved, we performed measurements of chain length dependence with a selected set of organic liquids (Figures 3–5). In these experiments, we compared bottom electrodes of Ag^{TS} to Au^{TS} , values of J_0 (at ± 0.5 V), and the value of β generated by these sets of measurements against control experiments performed in air. Since SAMs on Au^{TS} are less tightly packed than on Ag^{TS}, the use of these two bottom electrodes allowed us to compare a controlled variation in the structure of the SAMs that was independent of the effect of the liquid. SAMs of nalkanethiolates are more vertically oriented with respect to the surface on silver (with a tilt angle, $\theta = 11^{\circ}$) than on gold (θ = 31°) (and thus, in principle, there is less potential for the intercalation of molecules from the liquid phase in between the chains) but have similar values of J_0 and β (suggesting similar pathways of tunneling, i.e., through bond tunneling). These control experiments allow us to distinguish and characterize different types of interactions between the SAMs and liquids included in the junctions. We note here that the shape of the I(V) curves for different liquids are all symmetrical, and we do not observe current rectification at ± 0.5 V. (See the values of all averaged I(V) curves in the Supporting Information.)

Air (I). As a control, we first determined the values of β and J_0 for SAMs of SC_n (with n=4,6,8...,18) with the EGaIn junction in air, using previously reported procedures. The dashed lines in Figure 3 show a fit of $\log(J)$ at -0.5 V as a function of n to eq 1. The values of J(V), J_0 , and β for SAMs supported by Ag^{TS} and Au^{TS} measured in air reported here are statistically indistinguishable from the values reported

previously.^{28,76,77} The agreement in the values of β (~1.0 $n_{\rm C}^{-1}$) among these measurements confirms the "high" quality of the *n*-alkanethiolate SAM-based junctions.⁷⁶

Perfluorocarbons (II). Measurements of tunneling currents across alkanethiolate SAMs as a function of chain length in liquids of perfluorocarbons gave similar results to measurements conducted in air (Figure 3A–D). From these results, we inferred that the perfluorocarbon molecules do not intercalate into the monolayer or form a surface film with either the SAM or Ga₂O₃ surface. These results demonstrate that (i) if the liquid does not interact with SAMs, it does not contribute to the tunneling current density of SAMs. (ii) Since the perfluorocarbons are liquids, and are more viscous than air, ⁷⁸ these results indicate that the viscosity in the medium surrounding the junctions does not influence the tunneling current

Although there is no evidence for interactions as measured by tunneling current, perfluorocarbon liquids do seem to stabilize *n*-alkanethiolate SAMs against short circuiting between -0.5 and +0.5 V. We did not observe a single short after measuring more than 100 junctions in perfluorocarbons (see Table S1 in the Supporting Information for relevant statistics). In comparison, the corresponding numbers of failures in air would typically be 10 out of 100 junctions. While the mechanism of junction stabilization is not clear, it is possible that perfluorocarbons fill defective sites in the SAM and prevent short-circuit contacts between the top and bottom electrodes.⁷⁹ Regardless of the mechanism, we believe that measurements performed in perfluorocarbons have the potential to improve the stability of SAM-based junctions.

Comparison between junctions on both Ag^{TS} and Au^{TS} electrodes shows a small decrease in β ($\beta_{Ag} = 1.01 \pm 0.01$ C⁻¹

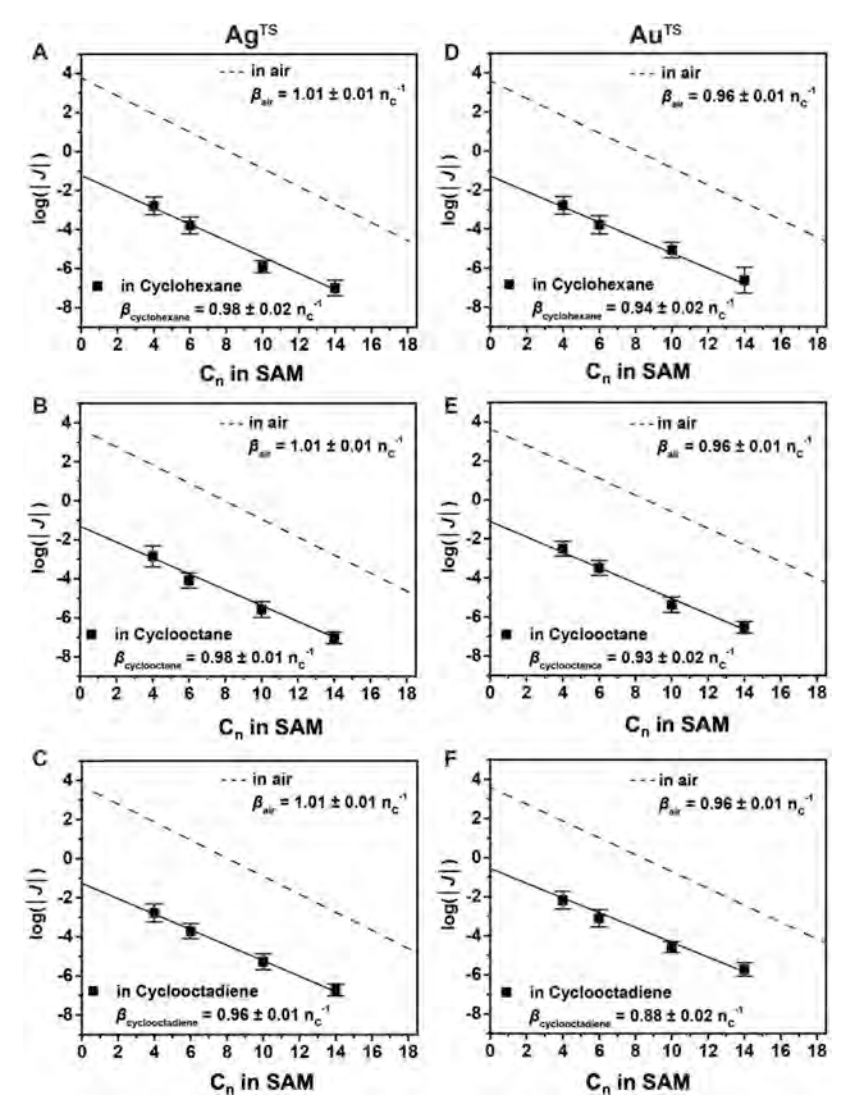


Figure 5. Plot of the Gaussian mean values of log(|JI|) at -0.5 V against the repeating carbon number n. The dashed lines are the J(V) measured in air, and the solid squares are measured in cyclohexane (A,D), cyclooctane (B,E), or cyclooctadiene (C,F). The error bars represent the standard deviation of the Gaussian mean values, and the solid lines are the Simmons equation fit to the data.

and $\beta_{\rm Au}=0.96\pm0.01~{\rm C}^{-1}).$ This difference is comparable with a small difference we measured before with junctions in air (in air: $\beta_{\rm Ag}=1.00\pm0.01~{\rm C}^{-1}$ and $\beta_{\rm Au}=0.92\pm0.02~{\rm C}^{-1}).^{32,76}$ We attribute the small difference in β to the difference in the supramolecular structure of SAMs formed on ${\rm Au^{TS}}$ vs ${\rm Ag^{TS}}$: (i) SAMs on ${\rm Au^{TS}}$ (tilt angle $\theta\sim30^\circ$) tilt more relative to the surface than that on ${\rm Ag^{TS}}$ ($\theta\sim10^\circ$) and (ii) the surface coverage of SAMs on ${\rm Au^{TS}}$ is about 10% less than that on ${\rm Ag^{TS}}$.

Charge Transport in Linear Hydrocarbons (III). Linear hydrocarbons (n-alkanes with n=6, 10, and 16) have the potential to interact with SAMs by intercalation within the monolayer or by layering on its surface. The results obtained from SAMs on silver and gold substrates under linear hydrocarbons are similar: the extrapolated values of J_0 for junctions immersed in hexane or hexadecane are very similar to those in contact with air (Figure 4A–D). The values of β from junctions immersed in liquid hydrocarbons are, however, markedly different: β changes from 1.01 $n_{\rm C}^{-1}$ in air to 1.33–1.39 $n_{\rm C}^{-1}$ (1.60–1.67 Å⁻¹) under linear hydrocarbons for Ag^{TS} and from 0.96 $n_{\rm C}^{-1}$ in air to 1.31 $n_{\rm C}^{-1}$ (1.57 Å⁻¹) for Au^{TS}. (For reference, the value of β for vacuum between two

electrodes separated by 1 nm is reported to be ~2.8 to 3.1 Å⁻¹.) Thus, the hydrocarbon liquid causes a larger reduction in tunneling currents for SAMs of longer chain length. There are two possible mechanisms for this effect: (i) the transition from liquid-like SAMs ($C_n < 10$) to crystalline-like SAMs ($C_n > 10$) could increase the order of the liquid film formed on the surface of the SAM and result in a thicker film or (ii) the solvent molecules could intercalate into the SAMs of longer chain length and disrupt through-bond charge tunneling.

Cyclic Hydrocarbons (IV). Compared to linear hydrocarbons, cyclic hydrocarbons are entirely different in their influence on the chain length dependence of the charge transport characteristics in these junctions. Their values of β are similar to those in air, but the curves (Figure 5; solid and dashed lines), although approximately parallel, are separated by 10^4 to 10^5 A/cm². This substantial difference in current density between the measurements in air and in cyclohexane (Figure 5A,D), cyclooctane (Figure 5B,E), and cyclooctandiene (Figure 5C,F) was initially unexpected but is compatible with the formation of a thin film of liquid at the surface of the SAM. Assuming that this hypothesis is correct, the following questions arise: (i) how thick is the liquid film formed by cyclic

hydrocarbons? (ii) What is the driving force for the adsorption of solvent molecules—interactions between liquid/Ga₂O₃ or liquid/SAMs or both? To understand better the liquid film we believe to be trapped in the junctions, we performed (and describe in the following sections) (i) an analysis of $\log(|J_0|)$ and β as a function of liquids and bottom electrodes, (ii) a comparison of the current density measured from the SAM of Ag^{TS}-S(CH₂)₂(CF₂)₇CF₃ and Ag^{TS}-C₁₀ in liquids, (iii) an estimation of the thickness of the liquid films, and (iv) MD simulation of the solvation layer at the interface between a gold slab and the top surface of C_n SAMs (n = 6, 10, 18) immersed in hexane and cyclohexane.

Effect of Bottom Electrodes. Figure 6 shows the values of $log(|J_0|)$ and β obtained from a best fit of the Simmons

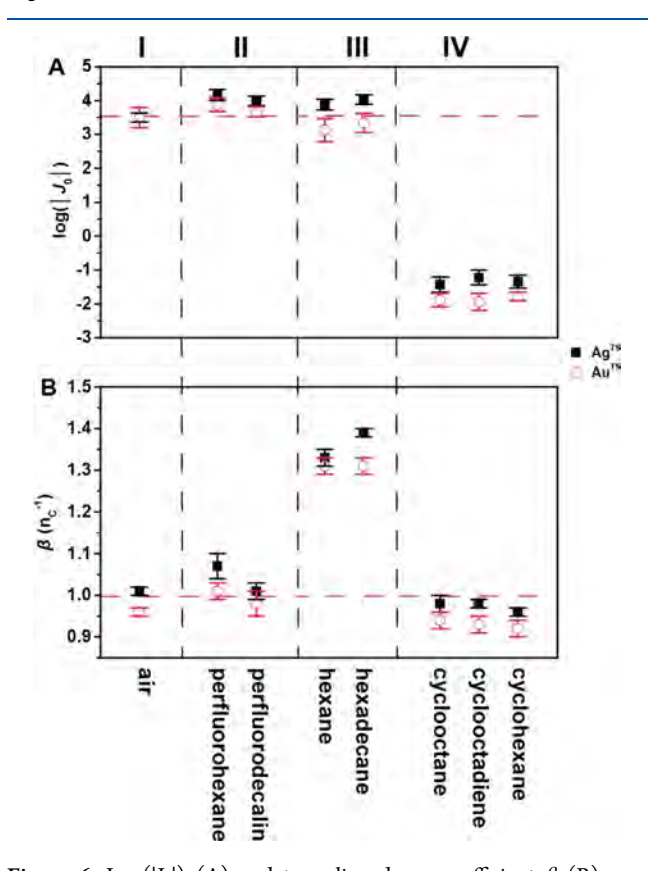


Figure 6. Log($|J_0|$) (A) and tunneling decay coefficient β (B) as a function of liquid measured with SAMs formed on Ag^{TS} (black solid square) and Au^{TS} (red solid dot). The black dashed lines separate the liquids in different catalogs as shown in Figure 1B. The red dashed lines are guide to eyes that illustrate the common values of β and $\log(J_0)$ measured with the SAMs of n-alkanethiolates in air using many testbeds. 5,76,80

equation (eq 1) to the experimental data as a function of selected organic liquids and bottom electrodes. We observed that the identity of the bottom electrode only produced small differences in $\log(|J_0|)$ and β . The values of $\log(|J_0|)$ for liquids in category IV are significantly lower than those in other liquids, which implies a large reduction of tunneling current at the interface of SAM/Ga₂O₃. In liquids of category IV, the difference in $\log(|J_0|)$ between SAMs on Ag^{TS} and Au^{TS} reflects a slight difference in the values of β (since it is obtained by extrapolation using the β of best fit). In liquids of type II and IV, the values of β are indistinguishable from those in contact with air and remain the same when Ag^{TS} or Au^{TS} bottom

electrodes are used. In liquids of type III, the values of β increase when SAMs are formed on Ag^{TS} or Au^{TS} . This difference in β suggests that there is either an increase in the height of the tunneling barrier or a gradient change in the width of the tunneling barrier with the number of carbons in the SAM. In a later section, we determine the width of the tunneling barrier of junctions in liquids and found out that the change in β can be accounted for by a gradient change in the width of the tunneling barrier with the number of carbons in the SAM. To further investigate the role of intermolecular forces on these observations, we measured charge transport through SAMs of $S(CH_2)_2(CF_2)_7CF_3$ under various solvents (Figure 7).

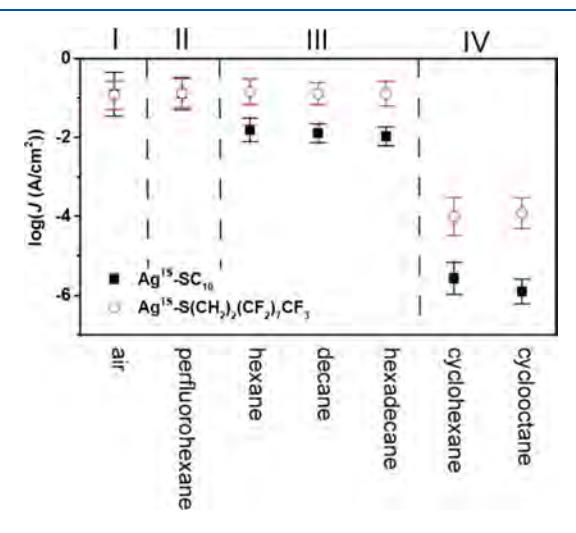


Figure 7. Plot of the Gaussian mean values of $\log(|J|)$ at -0.5~V measured with the SAMs of Ag^{TS} - SC_{10} (black solid square) and Ag^{TS} - $S(CH_2)_2(CF_2)_7CF_3$ (red solid dot) against different liquids. The dashed lines separate liquids in different groups.

Polyfluorinated SAMs Measured in Liquids. Figure 7 compares the values of log(IJI) measured from SAMs of AgTS- $S(CH_2)_2(CF_2)_7CF_3$ and $Ag^{TS}-SC_{10}$ under different perfluorocarbons and linear and cyclic hydrocarbons. We used polyfluorinated SAMs to alter the nature of the interactions between the liquid and SAM. We assume that hydrocarbons do not strongly interact with the SAMs of AgTS-S-(CH₂)₂(CF₂)₇CF₃), and we expected the values of current density to resemble those measured in air. In both perfluorocarbons and linear hydrocarbons, we found that the values of log(IJI) were statistically indistinguishable from junctions formed in air. When junctions were measured under cyclic hydrocarbons, however, the current density decreased by 3 orders of magnitude. This observation suggests that the liquid/SAM chemical interaction is not the sole reason for the current reduction in liquid of cyclic hydrocarbons, but the whole interface of SAM/liquid/Ga₂O₃ must be considered. Our data shows that there are nearly no linear hydrocarbons present during the charge transport measurements of the SAM of Ag^{TS}-S(CH₂)₂(CF₂)₇CF₃. This result suggests that linear hydrocarbons, which may be absorbed on the EGaIn tip and/ or the SAM of Ag^{TS} - $S(CH_2)_2(CF_2)_7CF_3$, can be "squeezed" out" upon bringing the EGaIn tip into contact with the SAM (corresponding to a pressure ~3-4 kPa).²⁶ Cyclic hydrocarbons, however, remain "trapped" in the junction and form a packed film between the EGaIn tip and the SAM.81

Table 1. Summary of Breakdown Measurements and Molecular Dimensions of Solvent Molecules

no.	liquid	$\log(J)$	$V_{\rm bd}({ m V})$	$d_{ m LF}$ estimated from $V_{ m bd}~({ m \AA})^a$	d_{LF}' estimated from $\log(J)$ $(\mathring{\mathrm{A}})^a$	a ^a (Å) ^b	l (Å)€	$n_{\rm layer}^{a}$
1	perfluorohexane	-0.9 ± 0.4	1.1 ± 0.1	0	0	4.9	10.5	0
7	hexane	-1.8 ± 0.3	1.4 ± 0.2	5.0 ± 0.5	4.8 ± 0.3	4.7	10.2	1
8	decane	-1.9 ± 0.2	1.4 ± 0.1	5.2 ± 0.4	5.0 ± 0.2	4.7	15.5	1
9	hexadecane	-2.0 ± 0.2	1.4 ± 0.2	5.4 ± 0.5	5.1 ± 0.2	4.7	23.1	1
10	cyclooctane	-5.6 ± 0.4	2.2 ± 0.2	15.2 ± 0.8	14.3 ± 0.6	5.5	8.6	2
12	cyclohexane	-5.9 ± 0.3	2.3 ± 0.3	15.7 ± 1.2	15.0 ± 0.5	5.0	8.0	3
15	benzene	-4.3 ± 0.2	1.9 ± 0.1	10.2 ± 0.4	10.0 ± 0.3	3.3	6.6	3
16	toluene	-4.2 ± 0.3	1.9 ± 0.2	10.9 ± 0.6	9.7 ± 0.3	3.8	8.2	3
23	trans,trans,cis-1,5,9-cyclododecatriene	-3.6 ± 0.4	1.6 ± 0.2	7.2 ± 0.5	8.3 ± 0.5	6.9	10.4	1
25	trans-decalin	-3.9 ± 0.4	1.6 ± 0.3	7.7 ± 1.0	8.5 ± 0.6	5.0	10.3	1
26	cis-decalin	-3.9 ± 0.5	1.7 ± 0.3	7.8 ± 2.5	8.5 ± 0.8	5.7	10.0	1
27	methylcyclopentadiene dimer	-2.8 ± 0.3	1.5 ± 0.2	6.0 ± 0.5	6.2 ± 0.3	5.5	9.1	1

 $^ad_{LF}$ calculated from eq 3, and d_{LF} calculated from eq 4. ba stands for the minimum dimension of a molecule that can pass a slit-shaped pore. Data are taken from refs 84 and. 85 $^dn_{layer}$ is estimated from the ratio of d_{LF}/a , d_{LF}/a , d_{LF}/a , defined as the thickness of the liquid film estimated from measurements of electrical breakdown.

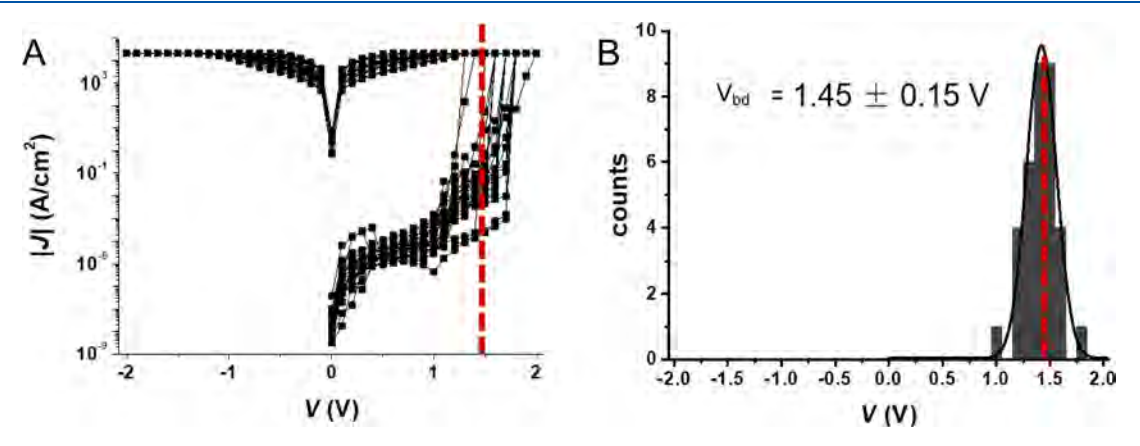


Figure 8. Measurements of electrical breakdown. (A) J(V) traces of a SC_{10} /hexane/ Ga_2O_3 /EGaIn junction as the voltage is increased to 2 V. (B) Histogram of the voltages at which the junctions short electrically, fitted with a Gaussian function. The dashed red line indicates the mean value of the breakdown voltage.

Measurements of Electrical Breakdown. To estimate the thickness of the liquid film in our tunneling junctions, we measured the voltage at which electrical breakdown $(V_{\rm bd})$ occurs. The total tunneling distance d (the sum of the thickness of the SAM and the thickness of a liquid film) can be calculated from eq 2, assuming that $E_{\rm bd}$ is a constant value of 0.81 GV/m.

$$d = (d_{SAM} + d_{LF}) = V_{bd}/E_{bd}$$
 (3)

where $d_{\rm SAM}$ (= 1.1 nm)^{82,83} is the thickness of the SAM of Ag-SC₁₀ measured by ellipsometry and XPS;^{32,36} $d_{\rm LF}$ is the thickness of the liquid film estimated from electrical breakdown measurement (see Table 1). The assumption that $E_{\rm bd}$ is the same for junctions with and without a liquid film can be restated as assuming that the voltage drop per unit length is the same for the liquid film and the SAM; this assumption is a rough approximation, and we expect that the voltage drop per unit length would be greater across the liquid layer due to the requirement for through-space tunneling, and thus, the thickness estimated in this way represents an upper bound for the true thickness of the junction.

The breakdown voltage as a function of liquid was determined as follows. First, a stable junction was formed with the SAM of SC_{10} in the selected liquid, and its J(V) characteristic was measured in the voltage window of ± 0.50 V

to verify that the J(V) curve fell within 1 standard deviation of the Gaussian log-mean J(V) curve. Next, we increased the voltage in either the positive or negative direction starting from 0 to +2.5 V or -2.5 V with a step of voltage of 0.05 V. At some voltage, the junction broke down abruptly. These voltages were characterized by a sharp increase of J of several orders of magnitude (see Figure 8A for examples). We repeated this experiment 30 times, and the $V_{\rm bd}$ values were plotted in histograms to which a Gaussian curve was fitted to determine the Gaussian average value of $V_{\rm bd}$ and its standard deviation (Figure 8B).

Estimation of Thickness from the Simmons Equation. We also estimated the thickness of the liquid film (assuming the formation of a liquid film in between the SAM and the surface of the EGaIn electrode) from the reduction in current density using a modified form of the Simmons equation

$$\frac{J_{\text{liq}}}{J_{\text{air}}} = \frac{J_{0}e^{-\beta(d'_{\text{LF}} + d_{\text{SAM}})}}{J_{0}e^{-\beta d_{\text{SAM}}}}$$
(4)

Here, $d_{\rm LF}{}'$ is the thickness of the liquid layer estimated by eq 4. Use of this equation requires the assumption that β is the same for the liquid film and the SAM; we expect that β is larger for the liquid film due to the requirement of through-space tunneling. Table 1 contains the calculated values of $d_{\rm LF}$ (from

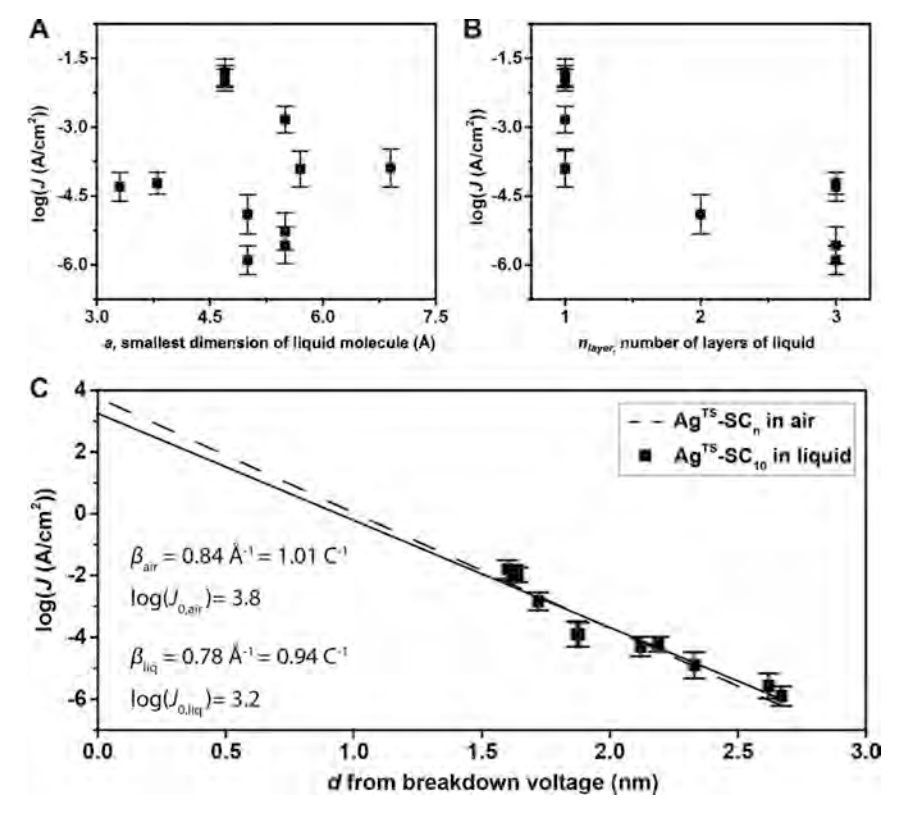


Figure 9. Plots of $\log(J)$ as a function of a (A), n_{layer} (B), and the tunneling distance (d) (C) estimated by the breakdown voltage. The solid line is the fit to the data of $\operatorname{Ag}^{TS}/\operatorname{SC}_{10}$ in liquid by eq 1. The thickness of the monolayer was estimated from dielectric breakdown experiments using eq 3. The molecules included in this analysis are listed in Table 1.

measurements of electrical breakdown) and $d_{\rm LF}$ (from the Simmons equation) for different liquids. The values of $d_{\rm LF}$ and $d_{\rm LF}$ estimated by different approaches are in good agreement. The fact that the values of $d_{\rm LF}$ obtained by analysis with the Simmons equation and by electrical breakdown measurements agree allows us to understand how the formation of a liquid film depends on the structure of the liquid molecules and liquid/SAM interactions.

The last three columns of Table 1 contain the dimensions of the liquid molecules calculated for each atom surrounded by a van der Waal sphere (~1.5 Å). Here, we used two critical dimensions: the shortest dimension, a (Å), and the longest dimension, l(A), of a molecule to account for the molecular shape and size. The value of a is the diameter of the smallest slit-shaped pore that the molecule can pass through and represents the minimum distance through a molecule. The value of l is the longest molecular dimension in the X-ray crystal structure of single crystals of these molecules. The values of a and $l_{\rm m}$ are taken from the literature. ^{84,85} Here, we observed that in many cases, the difference between the thickness of the monolayer and the thickness approximated by electrical breakdown measurements is compatible with the smallest dimension a of the liquid molecules. This result suggests that we can estimate the number of liquid layers (n_{laver}) see all data in Table 1) trapped in the junctions. For example, for hexane, $n_{\text{layer}} = 1$ ($d_{\text{LF}} = 5.0$ Å, a = 4.7 Å), and for cyclohexane, $n_{\text{layer}} = 2$ ($d_{\text{LF}} = 15.2$ Å, a = 5.5 Å), when the van der Waals distance (3 Å) between two cyclooctane layers is included. Our findings suggest that the liquid molecules lie flat (with their long axis parallel to the surface) at the interface between the surface of the SAM and Ga₂O₃, and they form ordered liquid films. In our junction system, an interesting

observation is that the linear and linear liquid molecules form one layer between the SAM and $\rm Ga_2O_3$ surfaces, and the cyclic liquid molecules form two to three layers of structured liquids.

Estimation of the Tunneling Decay Constant of the **Liquid Film** (β_L). Figure 9 shows the correlation between log(1 JI) and the values of a for the liquid molecules (listed in Table 1; Figure 9A, for a plot of log(|J|) as a function of l, see Figure S30 in the Supporting Information) to the number of molecules in the liquid layers (n_{layer}) and to the tunneling distance d. Here, we make three important observations. The values of log(IJI) do not correlate linearly with a (nor do they correlate linearly with l, Figure S30), so decreases in the tunneling current through junctions in liquid do not solely depend on the dimensions of liquid molecules. There is a weak correlation between the values of log(IJI) and n_{layer} (Figure 9B). Interestingly, a strong linear dependence between the values of log(IJI) and d is observed (Figure 9C). The values of d for the junctions in air are taken from our previous work.^{28,76} The distance-dependent tunneling decay coefficient of the current density through a thin film of liquid ($\beta_{\rm liq}=0.78~{\rm \AA}^{-1}$) is like that through SAMs of Ag^{TS}-SC_n ($\beta_{\rm SAM}=0.84~{\rm \AA}^{-1}$). This finding suggests that the liquid film generates a similar tunneling barrier to SAMs of Ag^{TS} -SC_n of equivalent thickness. The $\log(J_{0/\log}) = 3.2$ is similar to $\log(J_{0,\text{air}}) = 3.8$. In other words, the major source of the observed decrease in J through a liquid film and a SAM, compared to that through just the SAM in air, is the tunneling decay across the liquid film and not the van der Waals interface between the liquid film and the

Reanalysis of log(*J*) as a Function of Tunneling Distance. In Figure 10, we replot the data from Figure 4A for junctions immersed in hexane by replacing the independent

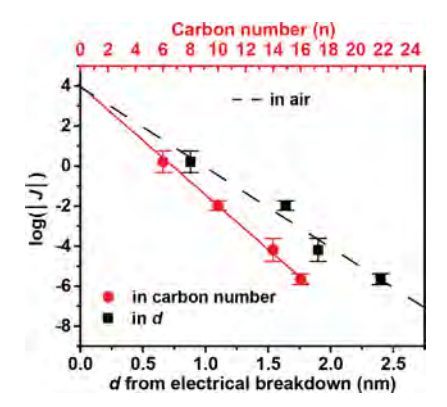


Figure 10. Plots of log(J) as a function of the tunneling distance (d) in hexane (C) estimated by the breakdown voltage. The red data points are the same from Figure 4A and correspond to the top axis. The black squares and dashed line correspond to the bottom axis and represent the tunneling distance inferred from measurements of the breakdown voltage.

variable of carbon number to tunneling distance $d = d_{\rm SAM} + d_{\rm LF}$ (estimated from the breakdown measurements). Plotted in this way, the current densities from junctions measured in hexane overlap with the junctions measured in air, and the $\beta_{\rm liq}$ (\sim 0.76

 ${\rm \AA}^{-1}$) is comparable to the $\beta_{\rm air}$ (0.84 ${\rm \AA}^{-1}$). From this observation, we interpret the results to indicate that the liquid film absorbed at the interface of SAM and ${\rm Ga_2O_3}$ increases the width of the tunneling barrier and in turn decreasing the measured current density.

MD Simulations. Figure 11 shows snapshots of the equilibrium dynamics of hexane (Figure 11A) and cyclohexane (Figure 11B) in the vicinity of SAMs of alkanethiolates as a gold slab is pushed toward the interface at a fixed pressure of 10⁵ kPa. We chose this value of pressure from an iterative approach, where the pressure was incrementally increased by orders of magnitude until we saw behavior that was consistent with the formation of structured liquid layers above the SAM. Interestingly, this value of pressure is approximately 4–5 orders of magnitude larger than the indirectly measured pressure of the EGaIn tip (using a cantilever). This difference is in agreement with several other measurements, which all suggest that the actual area of the EGaIn tip in contact with the SAM is 10⁻⁴ of the geometric area of the tip. ^{27,28}

In all simulations, we observed the formation of liquid layers with an increased density (relative to that of the bulk liquid) at the gold surface. In agreement with our inferences from electrical measurements, we observed that for SAMs of C_6 and C_{10} , the hexane molecules formed a monolayer liquid film,

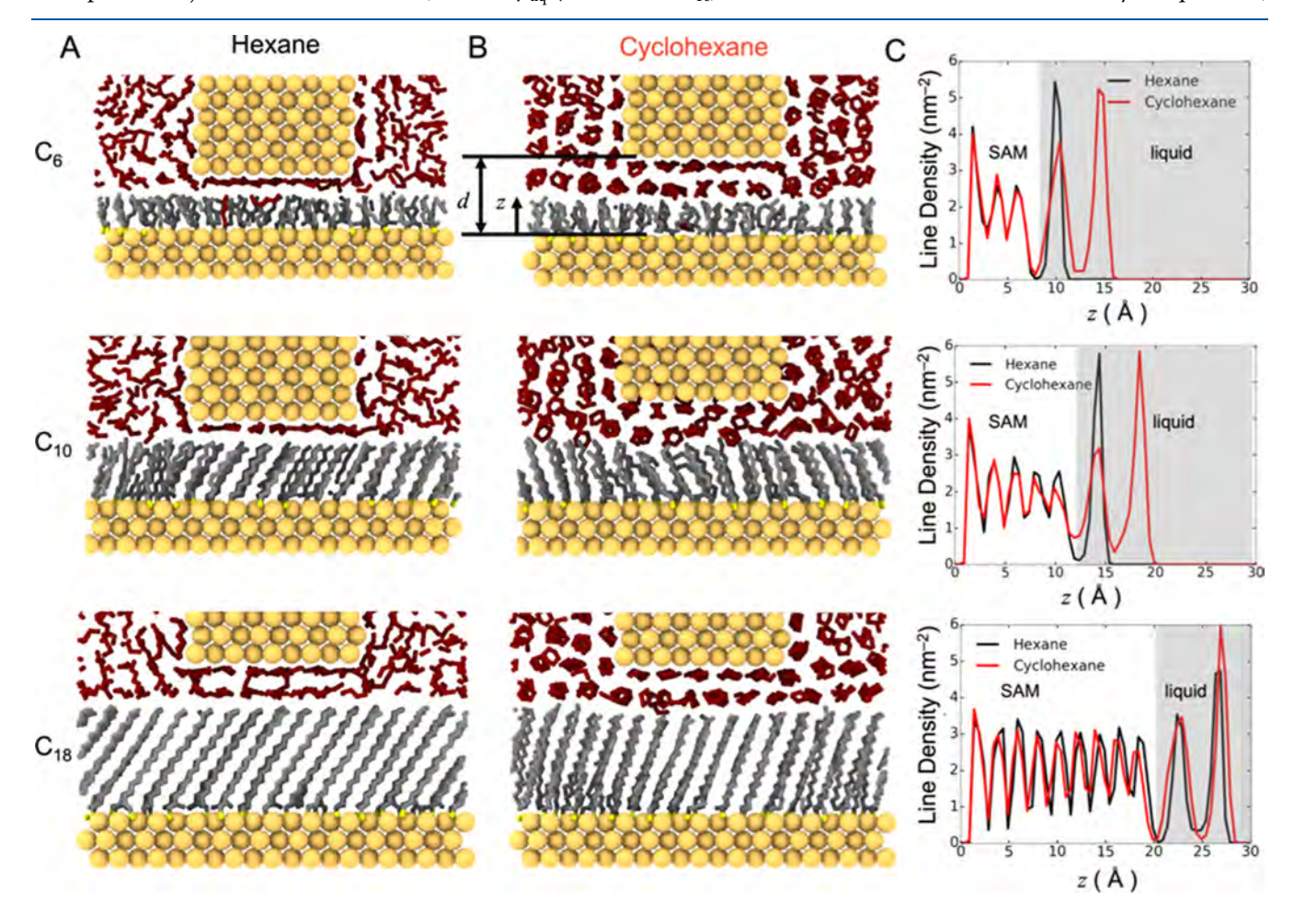


Figure 11. Results of MD simulations. Snapshots of a 2 nm cross section of a MD trajectory showing the equilibrium structure of (A) hexane and (B) cyclohexane molecules in the vicinity of alkanethiolate SAMs of various lengths ($C_n = 6$, 10, and 18) as a rigid block of gold atoms is pushed down toward the SAM at a constant pressure of 1.55×10^5 kPa. (C) Plot comparing the time-averaged (5 ns) line density of carbon atoms along the normal to the gold substrate for the equilibrated hexane and cyclohexane systems. The shaded regions of the plot indicate the contributions from the carbon atoms in the liquid film, and the unshaded regions indicate the contributions from carbon atoms in the SAM.

while the cyclohexane molecules formed a bilayer. For C₁₈ SAMs in contact with liquid hexane, we observed that two layers of hexane molecules persisted at equilibrium. It appears that the solid-like surface of the longer SAMs promotes the formation of ordered layers in the liquid, relative to the diffuse liquid-like surface of shorter SAMs. Moreover, the simulations showed that the solid-like C₁₈ SAMs were less prone to intercalation of hexane molecules than the shorter, liquid-like SAMs. We quantified our observations using the plots in Figure 11C, showing the line density of carbon atoms $(1/Å^2)$ as a function of distance from the gold surface. Taken together, these results suggest that, in linear alkanes, the apparent change in β was the result of a gradient change in the width of the tunneling barrier with the thickness of the monolayer, as opposed to a change in the height of the tunneling barrier (due to intercalation of molecules into the SAM). The fact that a step change is observed in the simulations, but no sharp transition is observable in the experimental data, probably reflects the idealized nature of the simulation, in comparison to the rough surface of Ga₂O₃ in the real system. We further note that since these simulations do not take into consideration grain boundaries in the AuTS and defects in the SAM, they cannot be used to probe associated phenomena, such as liquid molecules filling in defect sites; these phenomena would require more sophisticated simulations to describe.

CONCLUSIONS

These experimental results establish that the EGaIn electrode can be used to measure charge tunneling currents through SAMs immersed in non-polar solvents. Junctions formed in organic liquids demonstrate reductions in the rates of charge transport as a function of the liquid. We attribute to these reductions in current density to differences in the molecular structures of the liquids and to SAM/liquid/Ga $_2$ O $_3$ interactions. The sensitivity of this method to weak interactions (i.e., van der Waals interaction and electrostatic forces) provides insights into the interaction of liquids with the SAM/Ga $_2$ O $_3$ interface.

The physical-organic approach presented here varied all components of the system and interactions at interfaces and led to three conclusions. (i) Charge transport through junctions of the form of M^{TS} - SC_n //perfluorocarbon liquid// Ga₂O₃/EGaIn is like that in air. Thus, molecular junctions that are sensitive to oxidation, electromagnetic radiation, or air turbulence can be measured under degassed perfluorocarbons to diminish experimental uncertainties. (ii) For junctions measured under linear hydrocarbons, the reduction in current as a function of chain length results in an increase of the apparent β of the junctions, relative to β measured in air. Electrical breakdown measurements used to approximate the width of the tunneling barrier, as well as our MD simulations, suggest that this apparent change in β is the result of an additional liquid layer that forms on longer crystalline-like SAMs compared to shorter liquid-like SAMs. (iii) We observed a decrease in tunneling current density by a factor of $\sim 10^5$ for SAMs of SC_n—regardless of their length—when measured under cyclic hydrocarbons, relative to junctions measured in air. Their measured values of $\beta_{\text{cyclohexane}}$ (~1.0 n_{C}^{-1}), however, are statistically indistinguishable with that in air (β_{air}) , which leads to a $\sim 10^5$ times reduction in $\log(J_0)$, relative to junctions in air. We attribute this unexpectedly large and consistent decrease of J to be the result of a liquid film forming at the interface between the SAM and Ga₂O₃ surface (as opposed to

intercalation of the liquid molecules into the SAM), with the thickness of the liquid film being independent of the thickness of the SAMs.

We note that using the electrical breakdown measurements and the simplified Simmons equation model to estimate the structure and thickness of the liquid film is both based on an assumption that the ordered liquid film(s) forming in between the surfaces of SAMs and EGaIn electrode serves to increase the tunneling distance relative to direct contact between the EGaIn tip and the SAM in air/. There are also two other possibilities that are difficult to exclude: (1) the liquid molecules could fill in the defect sites of the SAMs to block leakage currents, resulting in a reduction of the measured tunneling current in liquids, and (2) the conductivity of the liquid film is unknown, and it could be much lower than we assumed. To examine the former possibility would require establishing a method to study the junction only at the defect sites of the SAMs. For the second possibility, we have attempted making direct contact with AuTS and EGaIn in hexane and cyclohexane, and both attempts yield only electrical shorts: without the SAM layer, the EGaIn tends to alloy with Au. These open questions remain interesting for further experimental and theoretical investigations.

Notwithstanding these limitations, our inference of the formation of mono- and multilayers of structured liquid films that resist expulsion between the contacting EGaIn/Ga2O3 and SAM interfaces is consistent with the existing measurements of molecular-scale oscillations in the force versus displacement curves obtained when two flat surfaces are brought together in a liquid environment using the SFA. While it is difficult to draw a direct correlation between our results and those of the SFA due to differences in the experimental techniques (i.e., direct measurement of a force trace at a constant rate of displacement vs inference of the equilibrium distance between the two surfaces of electrodes brought together at a fixed pressure of ~2 kPa²⁶ from measured changes in tunneling currents), our results provide additional empirical evidence to contribute to the theory of nanoscale solid-liquid-solid interfaces. 10 Moreover, the experimental simplicity of our approach, in comparison to the SFA, makes it easier to perform physical-organic experiments with a wider range of liquid molecules. Overall, we believe that measurements of rates of charge tunneling with the EGaIn junction immersed in liquids can be used as a new form of very-near surface analysis to examine the interactions between liquids and SAMs to characterize SAMs in liquids and to explore new relations between tunneling and (supra)molecular structure.

ASSOCIATED CONTENT

5 Supporting Information

The Supporting Information is available free of charge at https://pubs.acs.org/doi/10.1021/acs.jpcb.2c07901.

Overview of structured liquid films between two solid surfaces, experimental methods including materials, measurement, fabrication, and methods for statistical analysis, and statistics of electrical measurements (PDF)

AUTHOR INFORMATION

Corresponding Author

George M. Whitesides – Department of Chemistry and Chemical Biology, Harvard University, Cambridge, Massachusetts 02138, United States; Occid.org/0000-

0001-9451-2442; Email: gwhitesides@gmwgroup.harvard.edu

Authors

- Yuan Li Department of Chemistry, Tsinghua University, Beijing 100086, China; Department of Chemistry and Chemical Biology, Harvard University, Cambridge, Massachusetts 02138, United States
- Samuel E. Root Department of Chemistry and Chemical Biology, Harvard University, Cambridge, Massachusetts 02138, United States
- Lee Belding Department of Chemistry and Chemical Biology, Harvard University, Cambridge, Massachusetts 02138, United States
- Junwoo Park Department of Chemistry and Chemical Biology, Harvard University, Cambridge, Massachusetts 02138, United States; Department of Chemistry, Sogang University, Seoul 04107, Korea
- **Hyo Jae Yoon** Department of Chemistry, Korea University, Seoul 02841, Korea; orcid.org/0000-0002-2501-0251
- Cancan Huang Department of Chemistry and Chemical Biology, Harvard University, Cambridge, Massachusetts 02138, United States
- Mostafa Baghbanzadeh Department of Chemistry and Chemical Biology, Harvard University, Cambridge, Massachusetts 02138, United States; □ orcid.org/0000-0001-7678-1681

Complete contact information is available at: https://pubs.acs.org/10.1021/acs.jpcb.2c07901

Author Contributions

¹Y.L. and S.E.R. contributed equally.

Notes

The authors declare no competing financial interest.

ACKNOWLEDGMENTS

This work was supported by the National Science Foundation (NSF) award CHE-1808361. Characterization of the samples was performed in part at the Center for Nanoscale Systems (CNS) at Harvard University, a member of the National Nanotechnology Infrastructure Network (NNIN), which is supported by the NSF (ECS-0335765). Computational resources to support this work were provided by the Extreme Science and Engineering Discovery Environment (XSEDE) Program through the NSF grant number ACI-1053575, ⁸⁶ using the Comet supercomputer at the San Diego Supercomputer Center, with allocation DMR180105.

REFERENCES

- (1) Weiss, E. A.; Kaufman, G. K.; Kriebel, J. K.; Li, Z.; Schalek, R.; Whitesides, G. M. Si/SiO2-Templated formation of ultraflat metal surfaces on glass, polymer, and solder supports: Their use as substrates for self-assembled monolayers. *Langmuir* **2007**, 23, 9686–9694.
- (2) Jiang, L.; Wang, T.; Nijhuis, C. A. Fabrication of ultra-flat silver surfaces with sub-micro-meter scale grains. *Thin Solid Films* **2015**, 593, 26–39.
- (3) Chiechi, R. C.; Weiss, E. A.; Dickey, M. D.; Whitesides, G. M. Eutectic gallium-indium (EGaIn): A moldable liquid metal for electrical characterization of self-assembled monolayers. *Angew. Chem., Int. Ed.* **2008**, *47*, 142–144.
- (4) Barber, J. R.; Yoon, H. J.; Bowers, C. M.; Thuo, M. M.; Breiten, B.; Gooding, D. M.; Whitesides, G. M. Influence of environment on

- the measurement of rates of charge transport across Ag^{TS}/SAM//Ga₂O₃/EGaln Junctions. *Chem. Mater.* **2014**, *26*, 3938–3947.
- (5) Nijhuis, C. A.; Reus, W. F.; Barber, J. R.; Whitesides, G. M. Comparison of SAM-based junctions with Ga₂O₃/EGaln top electrodes to other large-area tunneling junctions. *J. Phys. Chem. C* **2012**, *116*, 14139–14150.
- (6) Li, Y.; Root, S. E.; Belding, L.; Park, J.; Rawson, J.; Yoon, H. J.; Baghbanzadeh, M.; Rothemund, P.; Whitesides, G. M. Characterizing chelation at surfaces by charge tunneling. *J. Am. Chem. Soc.* **2021**, *143*, 5967–5977.
- (7) Kumar, K. S.; Pasula, R. R.; Lim, S.; Nijhuis, C. A. Long-range tunneling processes across ferritin-based junctions. *Adv. Mater.* **2016**, 28, 1824–1830.
- (8) Amdursky, N.; Ferber, D.; Pecht, I.; Sheves, M.; Cahen, D. Redox activity distinguishes solid-state electron transport from solution-based electron transfer in a natural and artificial protein: cytochrome C and hemin-doped human serum albumin. *Phys. Chem. Chem. Phys.* **2013**, *15*, 17142–17149.
- (9) Bai, J.; Daaoub, A.; Sangtarash, S.; Li, X.; Tang, Y.; Zou, Q.; Sadeghi, H.; Liu, S.; Huang, X.; Tan, Z.; et al. Anti-resonance features of destructive quantum interference in single-molecule thiophene junctions achieved by electrochemical gating. *Nat. Mater.* **2019**, *18*, 364–369.
- (10) Israelachvili, J. N.Intermolecular and Surface Forces, 3rd ed.; Academic Press: San Diego, CA, USA, 2011.
- (11) Israelachvili, J.; Pashley, R. The hydrophobic interaction is long range, decaying exponentially with distance. *Nature* **1982**, *300*, 341.
- (12) Tabor, D.; Winterton, R. H. S. The direct measurement of normal and retarded van der Waals forces. *Proc. R. Soc. London, Ser. A* 1969, 312, 435–450.
- (13) Christenson, H. K.; Claesson, P. M. Direct measurements of the force between hydrophobic surfaces in water. *Adv. Colloid Interface Sci.* **2001**, *91*, 391–436.
- (14) Claesson, P. M.; Christenson, H. K. Very long range attractive forces between uncharged hydrocarbon and fluorocarbon surfaces in water. *J. Phys. Chem.* **1988**, 92, 1650–1655.
- (15) Klein, J. Forces between mica surfaces bearing adsorbed macromolecules in liquid media. *J. Chem. Soc., Faraday Trans. 1* **1983**, 79, 99–118.
- (16) Klein, J. Forces between mica surfaces bearing layers of adsorbed polystyrene in cyclohexane. *Nature* **1980**, 288, 248–250.
- (17) Parker, J. L.; Christenson, H. K.; Ninham, B. W. Device for measuring the force and separation between two surfaces down to molecular separations. *Rev. Sci. Instrum.* **1989**, *60*, 3135–3138.
- (18) Briscoe, W. H.; Horn, R. G. Direct measurement of surface forces due to charging of solids immersed in a nonpolar liquid. *Langmuir* **2002**, *18*, 3945–3956.
- (19) Tonck, A.; Georges, J. M.; Loubet, J. L. Measurements of intermolecular forces and the rheology of dodecane between alumina surfaces. *J. Colloid Interface Sci.* **1988**, *126*, 150–163.
- (20) Heuberger, M. The extended surface forces apparatus. Part I. Fast spectral correlation interferometry. *Rev. Sci. Instrum.* **2001**, *72*, 1700–1707.
- (21) Weiss, E. A.; Chiechi, R. C.; Kaufman, G. K.; Kriebel, J. K.; Li, Z. F.; Duati, M.; Rampi, M. A.; Whitesides, G. M. Influence of defects on the electrical characteristics of mercury-drop junctions: Self-assembled monolayers of n-alkanethiolates on rough and smooth silver. J. Am. Chem. Soc. 2007, 129, 4336–4349.
- (22) Yuan, L.; Nerngchamnong, N.; Cao, L.; Hamoudi, H.; del Barco, E.; Roemer, M.; Sriramula, R. K.; Thompson, D.; Nijhuis, C. A. Controlling the direction of rectification in a molecular diode. *Nat. Commun.* **2015**, *6*, 6324.
- (23) Fracasso, D.; Valkenier, H.; Hummelen, J. C.; Solomon, G. C.; Chiechi, R. C. Evidence for quantum interference in SAMs of arylethynylene thiolates in tunneling junctions with eutectic Ga—In (EGaIn) top-contacts. *J. Am. Chem. Soc.* **2011**, *133*, 9556—9563.
- (24) Kong, G. D.; Kim, M.; Cho, S. J.; Yoon, H. J. Gradients of rectification: Tuning molecular electronic devices by the controlled

- use of different-sized diluents in heterogeneous self-assembled monolayers. *Angew. Chem., Int. Ed.* **2016**, *55*, 10307–10311.
- (25) Chen, J.; Kim, M.; Gathiaka, S.; Cho, S. J.; Kundu, S.; Yoon, H. J.; Thuo, M. M. Understanding keesom interactions in monolayer-based large-area tunneling junctions. *J. Phys. Chem. Lett.* **2018**, 9, 5078–5085.
- (26) Rothemund, P.; Morris Bowers, C.; Suo, Z.; Whitesides, G. M. Influence of the contact area on the current density across molecular tunneling junctions measured with EGaIn top-electrodes. *Chem. Mater.* **2018**, *30*, 129–137.
- (27) Du, W.; Wang, T.; Chu, H.-S.; Wu, L.; Liu, R.; Sun, S.; Phua, W. K.; Wang, L.; Tomczak, N.; Nijhuis, C. A. On-chip molecular electronic plasmon sources based on self-assembled monolayer tunnel junctions. *Nat. Photonics* **2016**, *10*, 274–280.
- (28) Simeone, F. C.; Yoon, H. J.; Thuo, M. M.; Barber, J. R.; Smith, B.; Whitesides, G. M. Defining the value of injection current and effective electrical contact area for egaln-based molecular tunneling junctions. *J. Am. Chem. Soc.* **2013**, *135*, 18131–18144.
- (29) Wang, G.; Kim, T. W.; Lee, H.; Lee, T. Influence of metal-molecule contacts on decay coefficients and specific contact resistances in molecular junctions. *Phys. Rev. B: Condens. Matter Mater. Phys.* **2007**, *76*, 205320–205417.
- (30) Baghbanzadeh, M.; Bowers, C. M.; Rappoport, D.; Żaba, T.; Yuan, L.; Kang, K.; Liao, K.-C.; Gonidec, M.; Rothemund, P.; Cyganik, P.; et al. Anomalously rapid tunneling: Charge transport across self-assembled monolayers of oligo(ethylene glycol). *J. Am. Chem. Soc.* **2017**, *139*, 7624–7631.
- (31) Bowers, C. M.; Liao, K.-C.; Yoon, H. J.; Rappoport, D.; Baghbanzadeh, M.; Simeone, F. C.; Whitesides, G. M. Introducing ionic and/or hydrogen bonds into the SAM//Ga₂O₃ top-interface of Ag^{TS}/S(CH₂)_nT//Ga₂O₃/EGaIn junctions. *Nano Lett.* **2014**, *14*, 3521–3526.
- (32) Baghbanzadeh, M.; Simeone, F. C.; Bowers, C. M.; Liao, K.-C.; Thuo, M.; Baghbanzadeh, M.; Miller, M. S.; Carmichael, T. B.; Whitesides, G. M. Odd—even effects in charge transport across nalkanethiolate-based SAMs. *J. Am. Chem. Soc.* **2014**, *136*, 16919—16925.
- (33) Yoon, H. J.; Shapiro, N. D.; Park, K. M.; Thuo, M. M.; Soh, S.; Whitesides, G. M. The Rate of Charge tunneling through self-assembled monolayers is insensitive to many functional group substitutions. *Angew. Chem., Int. Ed.* **2012**, *51*, 4658–4661.
- (34) Nijhuis, C. A.; Reus, W. F.; Whitesides, G. M. Molecular rectification in metal-sam-metal oxide-metal junctions. *J. Am. Chem. Soc.* **2009**, *131*, 17814–17827.
- (35) Valtiner, M.; Donaldson, S. H.; Gebbie, M. A.; Israelachvili, J. N. Hydrophobic Forces, Electrostatic steering, and acid—base bridging between atomically smooth self-assembled monolayers and end-functionalized PEGolated lipid bilayers. *J. Am. Chem. Soc.* **2012**, 134, 1746—1753.
- (36) Zeng, H.; Tian, Y.; Zhao, B.; Tirrell, M.; Israelachvili, J. Friction at the liquid/liquid interface of two immiscible polymer films. *Langmuir* **2009**, *25*, 4954–4964.
- (37) Thompson, P. A.; Brinckerhoff, W. B.; Robbins, M. O. Microscopic studies of static and dynamic contact angles. *J. Adhes. Sci. Technol.* **1993**, *7* (6), 535–554.
- (38) Israelachvili, J; McGuiggan, P; Gee, M; Homola, A; Robbins, M; Thompson, P Liquid dynamics in molecularly thin films. *J. Phys.: Condens. Matter* **1990**, 2 (S), SA89.
- (39) Laibinis, P. E.; Whitesides, G. M.; Allara, D. L.; Tao, Y. T.; Parikh, A. N.; Nuzzo, R. G. Comparison of the structures and wetting properties of self-assembled monolayers of normal-alkanethiols on the coinage metal-surfaces, Cu, Ag, Au. *J. Am. Chem. Soc.* **1991**, *113*, 7152–7167.
- (40) Israelachvili, J.; Min, Y.; Akbulut, M.; Alig, A.; Carver, G.; Greene, W.; Kristiansen, K.; Meyer, E.; Pesika, N.; Rosenberg, K.; et al. Recent advances in the surface forces apparatus (SFA) technique. *Rep. Prog. Phys.* **2010**, *73*, 036601.
- (41) Haag, R.; Rampi, M. A.; Holmlin, R. E.; Whitesides, G. M. Electrical breakdown of aliphatic and aromatic self-assembled

- monolayers used as nanometer-thick organic dielectrics. J. Am. Chem. Soc. 1999, 121, 7895–7906.
- (42) Esplandiu, M. J.; Carot, M. L.; Cometto, F. P.; Macagno, V. A.; Patrito, E. M. Electrochemical STM investigation of 1,8-octanedithiol monolayers on Au(111). Experimental and theoretical study. *Surf. Sci.* **2006**, *600*, 155–172.
- (43) Xu, B. Q.; Tao, N. J. J. Measurement of single-molecule resistance by repeated formation of molecular junctions. *Science* **2003**, 301, 1221–1223.
- (44) Nichols, R. J.; Higgins, S. J. Single-molecule electronics: Chemical and analytical perspectives. *Annu. Rev. Anal. Chem.* **2015**, *8*, 389–417.
- (45) Li, X.; He, J.; Hihath, J.; Xu, B.; Lindsay, S. M.; Tao, N. Conductance of single alkanedithiols: conduction mechanism and effect of molecule–electrode contacts. *J. Am. Chem. Soc.* **2006**, *128*, 2135–2141.
- (46) Choi, B.; Capozzi, B.; Ahn, S.; Turkiewicz, A.; Lovat, G.; Nuckolls, C.; Steigerwald, M. L.; Venkataraman, L.; Roy, X. Solvent-dependent conductance decay constants in single cluster junctions. *Chem. Sci.* **2016**, *7*, 2701–2705.
- (47) Kim, T. W.; Wang, G. N.; Lee, H.; Lee, T. Statistical analysis of electronic properties of alkanethiols in metal-molecule-metal junctions. *Nanotechnology* **2007**, *18*, 315204–315211.
- (48) Wang, G.; Kim, Y.; Choe, M.; Kim, T. W.; Lee, T. A new approach for molecular electronic junctions with a multilayer graphene electrode. *Adv. Mater.* **2011**, *23*, 755–760.
- (49) Akkerman, H. B.; Naber, R. C. G.; Jongbloed, B.; van Hal, P. A.; Blom, P. W. M.; de Leeuw, D. M.; de Boer, B. Electron tunneling through alkanedithiol self-assembled monolayers in large-area molecular junctions. *Proc. Natl. Acad. Sci. U.S.A.* **2007**, *104*, 11161–11166.
- (50) Puebla-Hellmann, G.; Venkatesan, K.; Mayor, M.; Lörtscher, E. Metallic nanoparticle contacts for high-yield, ambient-stable molecular-monolayer devices. *Nature* **2018**, *559*, 232–235.
- (51) Chabinyc, M. L.; Chen, X. X.; Holmlin, R. E.; Jacobs, H.; Skulason, H.; Frisbie, C. D.; Mujica, V.; Ratner, M. A.; Rampi, M. A.; Whitesides, G. M. Molecular rectification in a metal-insulator-metal junction based on self-assembled monolayers. *J. Am. Chem. Soc.* **2002**, *124*, 11730–11736.
- (52) Holmlin, R. E.; Haag, R.; Chabinyc, M. L.; Ismagilov, R. F.; Cohen, A. E.; Terfort, A.; Rampi, M. A.; Whitesides, G. M. Electron transport through thin organic films in metal-insulator-metal junctions based on self-assembled monolayers. *J. Am. Chem. Soc.* **2001**, *123*, 5075–5085.
- (53) Simmons, J. G. Electric tunnel effect between dissimilar electrodes separated by a thin insulating film. *J. Appl. Phys.* **1963**, 34, 2581–2590.
- (54) Joachim, C.; Ratner, M. A. Molecular electronics: Some views on transport junctions and beyond. *Proc. Natl. Acad. Sci. U.S.A.* **2005**, *102*. 8801–8808.
- (55) Salomon, A.; Cahen, D.; Lindsay, S.; Tomfohr, J.; Engelkes, V. B.; Frisbie, C. D. Comparison of electronic transport measurements on organic molecules. *Adv. Mater.* **2003**, *15*, 1881–1890.
- (56) Park, S.; Kang, S.; Yoon, H. J. Power factor of one molecule thick films and length dependence. *ACS Cent. Sci.* **2019**, *5*, 1975–1982.
- (57) Yoon, H. J.; Bowers, C. M.; Baghbanzadeh, M.; Whitesides, G. M. The rate of charge tunneling is insensitive to polar terminal groups in self-assembled monolayers in $Ag^{TS}S(CH_2)_nM(CH_2)_mT$ // Ga_2O_3 / EGaIn Junctions. *J. Am. Chem. Soc.* **2014**, *136*, 16–19.
- (58) Holmlin, R. E.; Haag, R.; Chabinyc, M. L.; Ismagilov, R. F.; Cohen, A. E.; Terfort, A.; Rampi, M. A.; Whitesides, G. M. Electron transport through thin organic films in metal–insulator–metal junctions based on self-assembled monolayers. *J. Am. Chem. Soc.* **2001**, *123*, 5075–5085.
- (59) Akkerman, H. B.; de Boer, B. Electrical conduction through single molecules and self-assembled monolayers. *J. Phys. Condens. Matter* **2008**, *20*, 013001.

- (60) Simeone, F. C.; Yoon, H. J.; Thuo, M. M.; Barber, J. R.; Smith, B.; Whitesides, G. M. Defining the value of injection current and effective electrical contact area for egain-based molecular tunneling junctions. *J. Am. Chem. Soc.* **2013**, *135*, 18131–18144.
- (61) Chen, F.; Li, X. L.; Hihath, J.; Huang, Z. F.; Tao, N. J. Effect of anchoring groups on single-molecule conductance: comparative study of thiol-, amine-, and carboxylic-acid-terminated molecules. *J. Am. Chem. Soc.* **2006**, *128*, 15874–15881.
- (62) Dalvi, V. H.; Rossky, P. J. Molecular origins of fluorocarbon hydrophobicity. *Proc. Natl. Acad. Sci. U.S.A.* **2010**, *107*, 13603–13607.
- (63) Kahn, R.; Fourme, R.; André, D.; Renaud, M. Crystal structure of cyclohexane I and II. *Acta Crystallogr., Sect. B: Struct. Crystallogr. Cryst. Chem.* 1973, 29, 131–138.
- (64) Love, J. C.; Estroff, L. A.; Kriebel, J. K.; Nuzzo, R. G.; Whitesides, G. M. Self-assembled monolayers of thiolates on metals as a form of nanotechnology. *Chem. Rev.* **2005**, *105*, 1103–1170.
- (65) Rouhana, L. L.; Moussallem, M. D.; Schlenoff, J. B. Adsorption of short-chain thiols and disulfides onto gold under defined mass transport conditions: Coverage, kinetics, and mechanism. *J. Am. Chem. Soc.* **2011**, *133*, 16080–16091.
- (66) Nerngchamnong, N.; Yuan, L.; Qi, D. C.; Li, J.; Thompson, D.; Nijhuis, C. A. The role of van der Waals forces in the performance of molecular diodes. *Nat. Nanotechnol.* **2013**, *8*, 113–118.
- (67) Shpaisman, H.; Cohen, H.; Har-Lavan, R.; Azulai, D.; Stein, N.; Cahen, D. A novel method for investigating electrical breakdown enhancement by nm-sized features. *Nanoscale* **2012**, *4*, 3128–3134.
- (68) Yuan, L.; Li, J.; Nijhuis, C. A. The drive force of electrical breakdown of large-area molecular tunnel junctions. *Adv. Funct. Mater.* **2018**, 28, 1801710.
- (69) DiBenedetto, S. A.; Facchetti, A.; Ratner, M. A.; Marks, T. J. Charge conduction and breakdown mechanisms in self-assembled nanodielectrics. *J. Am. Chem. Soc.* **2009**, *131*, 7158–7168.
- (70) Zener, C. A Theory of the electrical breakdown of solid dielectrics. *Proc. R. Soc. London, Ser. A* 1934, 145, 523–529.
- (71) Song, H.; Lee, H.; Lee, T. Intermolecular chain-to-chain tunneling in metal-alkanethiol-metal junctions. *J. Am. Chem. Soc.* **2007**, *129*, 3806–3807.
- (72) Plimpton, S. Fast parallel algorithms for short-range molecular dynamics. *J. Comput. Phys.* **1995**, *117*, 1–19.
- (73) Stukowski, A. Visualization and analysis of atomistic simulation data with OVITO the Open visualization tool. *Modell. Simul. Mater. Sci. Eng.* **2010**, *18*, 015012.
- (74) Wang, J.; Wolf, R.; Caldwell, J.; Kollman, P.; Case, D. Development and testing of a general AMBER force field. *J. Comput. Chem.* **2004**, *25*, 1157–1174.
- (75) Ghorai, P. K.; Glotzer, S. C. Molecular dynamics simulation study of self-assembled monolayers of alkanethiol surfactants on spherical gold nanoparticles. *J. Phys. Chem. C* **2007**, *111*, 15857–15862.
- (76) Yuan, L.; Jiang, L.; Zhang, B.; Nijhuis, C. A. Dependency of the tunneling decay coefficient in molecular tunneling junctions on the topography of the bottom electrodes. *Angew. Chem., Int. Ed.* **2014**, *53*, 3377–3381.
- (77) Thuo, M. M.; Reus, W. F.; Nijhuis, C. A.; Barber, J. R.; Kim, C.; Schulz, M. D.; Whitesides, G. M. Odd-even effects in charge transport across self-assembled monolayers. *J. Am. Chem. Soc.* **2011**, *133*, 2962–2975.
- (78) Freire, M. G.; Ferreira, A. G. M.; Fonseca, I. M. A.; Marrucho, I. M.; Coutinho, J. A. P. Viscosities of liquid fluorocompounds. *J. Chem. Eng. Data* **2008**, *53*, *538*–*542*.
- (79) Scott, R. L. The solubility of fluorocarbons1. *J. Am. Chem. Soc.* **1948**, *70*, 4090–4093.
- (80) Vilan, A.; Aswal, D.; Cahen, D. Large-area, ensemble molecular electronics: Motivation and challenges. *Chem. Rev.* **2017**, *117*, 4248–4286.
- (81) Yarin, A. L. Drop impact dynamics: Splashing, spreading, receding, bouncing. *Annu. Rev. Fluid Mech.* **2006**, *38*, 159–192.
- (82) Jiang, L.; Sangeeth, C. S. S.; Yuan, L.; Thompson, D.; Nijhuis, C. A. One-nanometer thin monolayers remove the deleterious effect

- of substrate defects in molecular tunnel junctions. *Nano Lett.* **2015**, *15*, *6643*–*6649*.
- (83) Engelkes, V. B.; Beebe, J. M.; Frisbie, C. D. Length-dependent transport in molecular junctions based on SAMs of alkanethiols and alkanedithiols: Effect of metal work function and applied bias on tunneling efficiency and contact resistance. *J. Am. Chem. Soc.* **2004**, *126*, 14287–14296.
- (84) Tro, N. J.Chemistry: A Molecular Approach; Pearson: Boston, MA, 2014.
- (85) Lide, D. R.CRC Handbook of Chemistry and Physics; CRC Press: Boca Raton, FL, USA, 2004.
- (86) Towns, J.; Cockerill, T.; Dahan, M.; Foster, I.; Gaither, K.; Grimshaw, A.; Hazlewood, V.; Lathrop, S.; Lifka, D.; Peterson, G. D.; et al. XSEDE: Accelerating scientific discovery. *Comput. Sci. Eng.* **2014**, *16*, 62–74.

□ Recommended by ACS

Single-Molecule Human Nucleosome Spontaneously Ruptures under the Stress of Compressive Force: A New Perspective on Gene Stability and Epigenetic Pathways

Lalita Shahu, H. Peter Lu, et al.

DECEMBER 20, 2022

THE JOURNAL OF PHYSICAL CHEMISTRY B

READ 🗹

Biotin Binding Hardly Affects Electron Transport Efficiency across Streptavidin Solid-State Junctions

Sudipta Bera, David Cahen, et al.

JANUARY 17, 2023

LANGMUIR

READ 🗹

In Situ Confocal Raman Microscopy of Redox Polymer Films on Bulk Electrode Supports

Jiahe Xu, Carol Korzeniewski, et al.

JANUARY 13, 2023

ACS MEASUREMENT SCIENCE AU

READ [7

Mechanistic Study of the Conductance and Enhanced Single-Molecule Detection in a Polymer–Electrolyte Nanopore

Fabio Marcuccio, Martin Andrew Edwards, et al.

JANUARY 10, 2023

ACS NANOSCIENCE AU

READ 🗹

Get More Suggestions >